Journal of Drug Delivery Science and Technology 112 (2025) 107262

Contents lists available at ScienceDirect

Journal of Drug Delivery Science and Technology

journal homepage: www.elsevier.com/locate/jddst

Curcumin and resveratrol loaded in nanostructured mesoporous silica as a promising delivery system in Inflammatory Bowel Disease

Renan Stein [a,b], Miquel Martínez-Navarrete [c], Ana Paula Leão [a,b], Ana Melero [c], Silvio Buchner [d], Edilson Valmir Benvenutti [e], Monique Deon [f], Antonio José Guillot [c,*], Ruy Carlos Ruver Beck [a,b,**]

[a] Programa de Pós-Graduação em Ciências Farmacêuticas, Universidade Federal do Rio Grande do Sul, Av. Ipiranga, 2752, Porto Alegre, 90610-100, RS, Brazil
[b] Laboratório de Nanocarreadores e Impressão 3D em Tecnologia Farmacêutica (Nano3D), Faculdade de Farmácia, Universidade Federal do Rio Grande do Sul (UFRGS), Porto Alegre, 90610-100, RS, Brazil
[c] Department of Pharmacy and Pharmaceutical Technology and Parasitology, University of Valencia, Ave. Vicent Andrés Estellés s/n, 46100, Burjassot, Valencia, Spain
[d] Instituto de Física, Universidade Federal do Rio Grande do Sul, Porto Alegre, 91501970, RS, Brazil
[e] Instituto de Química, Universidade Federal do Rio Grande do Sul, Porto Alegre, 91501970, RS, Brazil
[f] Departamento de Farmacociências, Universidade Federal de Ciências da Saúde de Porto Alegre, Porto Alegre, 90050170, RS, Brazil

ARTICLE INFO

Keywords:
Mesoporous silica
Curcumin
Resveratrol and ulcerative colitis

ABSTRACT

Ulcerative colitis (UC) is a chronic inflammatory disease that significantly impacts mortality and morbidity worldwide. Unfortunately, there is no current curative treatment for this condition. Consequently, it is important to explore alternative treatment approaches. Polyphenols like resveratrol (RSV) and curcumin (CUR) could be good treatment candidates, due their pharmacological properties, such as strong antioxidant and anti-inflammatory activities. Despite their benefits, these compounds suffer from low solubility and intestinal permeability, resulting in their limited use in current therapies. In order to overcome the physico-chemical issues surrounding RSV and CUR, this work aims to encapsulate them in mesoporous silica particles (MS) as a strategy to improve their performances in the colitis treatment, using a mouse induced colitis model. The particles were in-house synthesised using tetraethyl orthosilicate (TEOS). RSV and CUR were successfully encapsulated separately into MS particles (drug loading 19 %). Mice were induced to UC using 3 % dextran sodium sulphate (DSS) added to the animals' water. The animals were treated for 7 days with sulfasalazine (100 mg/kg), free polyphenols (40 mg/kg), MS-CUR and MS-RSV (200 mg/kg) and blank particles (200 mg/kg). At the end of the treatments the colons were measured and their homogenates submitted to cytokines evaluation and histological analysis. Encapsulation in MS showed partial amorphization of polyphenols, which contributed to an increase in their solubility. The encapsulated polyphenols maintained the colon length/weight ratio in the animals, unlike free polyphenols ($p < 0.05$). In the same way, they were able to reduce the interleukins IL-1β and IL-6 ($p < 0.05$). These findings indicate that MS particles loaded with RSV and CUR are suitable for treating UC by reducing local inflammation.

1. Introduction

Ulcerative colitis (UC) is a complex and persistent Inflammatory Bowel Disease that occurs mainly due to a disorder of the epithelial barrier and immune responses, affecting 5 million people around the world [1]. Categorised as a chronic colonic condition, it mostly affects the descending colon, causing local irritation and inflammation, leading to moderate-to-severe symptoms like haematochezia, diarrhoea and abdominal pain [2]. Most cases of UC originate in the rectum and can progress throughout the colon. However, in some cases of proctitis, and left-sided colitis, there may be also an inflamed region near the entrance to the colon known as the caecum [3].

UC is a multifactorial disease without a fully understood origin, in which several extrinsic and intrinsic factors interact, including genetic

* Corresponding author. Department of Pharmacology, University of Valencia, Ave. Vicent Andrés Estellés s/n, 46100, Burjassot, Valencia, Spain.
** Corresponding author. Faculdade de Farmácia, Universidade Federal do Rio Grande do Sul, Av. Ipiranga 2752, Bairro Santana CEP, 90610-000, Porto Alegre, RS, Brazil.
E-mail addresses: antonio.guillot@uv.es (A.J. Guillot), ruy.beck@ufrgs.br (R.C.R. Beck).

https://doi.org/10.1016/j.jddst.2025.107262
Received 14 January 2025; Received in revised form 18 June 2025; Accepted 8 July 2025
Available online 9 July 2025

predisposition, environmental influences, altered composition of the gut microbiota and the reactivity of the intestinal immune system [4]. The chronic character of UC lies in a miscontrolled immune system reaction creating an inflammatory environment that reduces the mucin layer above the epithelial tissue, facilitates chemotaxis by increasing tight junctions, and contributes to a pathological adaptive immune response in the colon region mediated by neutrophils, macrophages and pro-inflammatory cytokines, such as IL-1β, IL-6 and TNF-α [5]. Although it can occur at any age, UC is most commonly diagnosed in individuals over the age of 55. Several studies have reported a rising incidence of the disease in many occidental countries, but also in developing countries in South America, Asia, Africa, and the Middle East. Current treatment protocols are largely palliative in nature [6].

Current standard treatments primarily aim to achieve symptom remission and involve the use of biological drugs, corticosteroids, and, most notably, aminosalicylates (5-ASA) such as mesalazine and sulfasalazine, which are considered the preferred first-line therapies [7]. Oral corticosteroids should be administered to patients that do not respond appropriately to 5-ASA, or to those with more severe symptoms and disease persistence, since they have demonstrated a superior effect in inducing remission of active UC. However, there is an issue related with corticosteroids after prolonged and continuous exposure to high doses, with adverse effects including weight loss, colon-rectal bleeding, acne, drowsiness, mood disorders, glucose intolerance and dyspepsia, causing more harm than benefit in about 50 % of cases [8].

Natural products, such as polyphenols, are bioactive substances widely recognised for their healthcare benefits, encompassing a broad range of compounds with multiple therapeutic properties [9]. Curcumin (CUR) and resveratrol (RSV), two representative polyphenolic compounds, are extracted from turmeric (*Curcuma longa* L.), and grapevines, berries, and pomegranate species, respectively. These polyphenols exhibit numerous biologically significant effects, including anti-inflammatory, neuroprotective, antioxidant, anticancer, anti-ageing, and cardiovascular protective properties [10–14]. Many reports recommend their use in the treatment of UC due to the ability of their metabolites to interact with local inflammation, reduce the production of interleukins, and promote proliferation of beneficial microorganisms, thereby helping to regulate the gut microbiota [15–18].

Despite their potential, both CUR and RSV have significant limitations due to their physicochemical characteristics, such as poor water solubility, instability at physiological pH, and extensive biotransformation via phase I and II reactions in enterocytes, liver, and intestinal microbiota, which greatly diminish their oral bioavailability [19,20]. For this reason, the development of advanced biomedical formulations to improve the physicochemical properties of these bioactive compounds has recently attracted the attention of many research groups. Concurrently, nanotechnology has increasingly been adopted to address these challenges. In this context, nanostructured Mesoporous Silica (MS) particles have gained particular prominence in the pharmaceutical field based on their ability to enhance the solubility, permeability, and physiological distribution of active ingredients [21–23].

MS particles, defined as inorganic materials composed of silicon dioxide, have been revealed as highly promising carriers for drug delivery, mainly thanks to the particular advantageous characteristics of silica. It is low in cost, has great superficial area and pore volume, and is biologically accepted and safe for use in the human body. This allows high levels of drug loading and targeting of drugs by functionalisation, with good biocompatibility [24–27]. Regardless of the particle size (micro or nano scale), the MS particles have a pore size ranging from 2 to 50 nm. This provides several advantages, for instance, enhanced drug solubility, thermal protection against degradation, and controlled drug release [28,29]. The application of distinct characterization techniques has shown that MS particles can improve the properties of active compounds by enhancing the wettability of poorly water-soluble drugs, stabilising them against hydrolysis, and improving the oral administration of hydrophobic active ingredients [30–33] such as RSV and CUR.

Therefore, this study aims to overcome the limitations of the polyphenols CUR and RSV through their incorporation into MS particles, followed by a comprehensive characterization of the particle systems. Subsequently, dextran sodium sulphate (DSS) was used to induce UC in mice and the *in vivo* effects of these novel treatments were determined by means of key evaluations: disease activity index (DAI) assessment, colon length and colon length-to-weight ratio measurements, cytokine levels, and histological analyses.

2. Materials and methods

2.1. Materials

Curcumin (CUR), 98 % tetraethyl orthosilicate (TEOS), hexadecyltrimethylammonium bromide (CTAB), acetone, polysorbate 80 (Tween 80), ethanol and trifluoroacetic acid were purchased from Sigma-Aldrich (São Paulo, Brazil). Resveratrol (RSV) was purchased from Purifarma (São Paulo, Brazil). Ammonia in solution (28 %) was purchased from Quimex (Uberaba, Brazil). HPLC grade acetonitrile and methanol were purchased from Merck (Darmstadt, Germany). Dextran Sodium Sulphate (DSS) and 3-aminophtalhydrazinde monosodium salt (luminol), were purchased from Sigma-Aldrich (St. Louis, USA). TNF-α, IL-4, IL-1β and IL-6 ELISA kits were acquired from Thermo Fisher Scientific (Waltham, USA). All other chemicals and solvents were of analytical grade and were used as received.

2.2. Synthesis of nanostructured MS particles

The synthesis of MS particles was performed by the method described by Grün et al. [34]. First, 1.6 g of CTAB was solubilised in a basic solution composed of 74 mL of ultrapure water and 6 mL of ammonia (28 % m/m) with controlled temperature (50 °C) and agitation. After 30 min, 7.6 mL of TEOS was added dropwise, and the reaction mixture remained under stirring and heating (50 °C) for 24 h. Subsequently, the reaction was transferred to a stainless-steel autoclave with a Teflon inner cup and subjected to a hydrothermal process in an oven at 100 °C for 24 h. Then, the MS particles were washed with ultrapure water, dried and calcined in a muffle furnace at 550 °C for 6 h to remove CTAB. The MS particles were stored in a desiccator to control humidity.

2.3. RSV and CUR loading

RSV and CUR were incorporated into MS using the incipient wetness method as follows [35]. A mixed solution of ethanol and acetone (50:50 ratio) was prepared, containing 40 mg/mL of each polyphenol separately. Then, 600 μL of this solution was added to 100 mg of previously dried MS, resulting in a polyphenol loading of 19.35 % (w/w). Afterwards, the materials were dried at 50 °C for 24 h and, finally, stored in a desiccator to control humidity. These particles were named MS-CUR and MS-RSV.

2.4. Extraction and HPLC method development

The extraction of polyphenols from MS-CUR and MS-RSV was performed using a solution of acetonitrile and acidified water pH 3 (60:40 v/v). Briefly, the samples were kept under stirring for 1 h at 600 RPM at room temperature and subsequently subjected to ultrasonication for 1 h. The content of polyphenol loaded in the particles was evaluated by High Performance Liquid Chromatography (HPLC) (Shimadzu System, Japan), according to a previously reported method [36]. For the analytical determination of CUR and RSV a RP-C18 column (250 × 4.6 mm; 5 μm; Phenomenex Gemini, Torrance, CA, USA) was used as the stationary phase. The mobile phase for RSV consisted in a mixture of methanol and acidified water pH 3 (60:40 v/v), delivered at a flow rate of 0.8 mL min^{-1} and detected at a wavelength of 306 nm. The mobile phase for CUR consisted in a mixture of acetonitrile and acidified water

pH 3 (60:40 v/v), delivered at a flow rate of 1.0 mL min^{-1} and detected at a wavelength of 427 nm. Both methods met the precision, specificity, accuracy and linearity in the range of 0.5–25 μg mL^{-1}.

2.5. N_2 adsorption and desorption

The textural characterization of MS before and after the incorporation of RSV and CUR was carried out through nitrogen adsorption analysis, using the Tristar II Kr 3020 equipment (Micromeritics, Georgia, USA). Before analysis, the samples were subjected to a degassing process at 60 °C for 12 h. The specific surface area was determined using the BET multipoint technique (Brunauer, Emmett and Teller), whereas the pore size distribution was obtained using the BJH method (Barret, Joyner and Halenda).

2.6. Thermal analysis

The MS, MS-CUR/RSV and non-encapsulated polyphenol samples were characterised in terms of thermal behaviour by differential scanning calorimetry (DSC) and thermogravimetric analysis (TGA). DSC analyses were performed using the DSC-60 equipment (Shimadzu, Kyoto, Japan), where a 5 mg sample contained in an aluminium pan was subjected to a heating rate of 10 °C min^{-1}, using nitrogen as purge gas (50 mL min^{-1}). Data were analysed using Lab Solution TA 60 software (Shimadzu, Kyoto, Japan). TGA analyses were performed using a TGA-50 thermoanalyser (Shimadzu, Kyoto, Japan), heating the samples in a platinum container up to 900 °C at a rate of 10 °C min^{-1}, under N_2 flow of 50 mL min^{-1}.

2.7. XRPD analysis

MS, MS-CUR/RSV and non-encapsulated polyphenols also had their X-ray diffraction profiles (XRPD) analysed by a Rigaku diffractometer (Tokyo, Japan), using Cu Kα (λ = 0.154056 nm) as a radiation source, a voltage of 40 kV, a current of 17 mA and a step of 0.05 in the range of 5–80 (2θ) and 1–10 (2θ).

2.8. FTIR analysis

For the Fourier-transform infrared spectroscopy (FTIR), 1 mg of samples of MS, MS-CUR, MS-RSV, and non-encapsulated polyphenols were mixed with 99 mg of potassium bromide (KBr). The samples were crushed in an agate mortar and pestle and finally pressed to obtain pellets (Ø = 1 cm). The spectra of the pellets were acquired using a Fourier transform IR Prestige21 infrared spectrophotometer (Shimadzu). The samples were evaluated in the spectral range of 500–4000 cm^{-1}.

2.9. TEM and SEM analysis

For transmission electron microscopy (TEM) analyses, the MS samples before and after polyphenol loading, were previously dispersed in isopropanol and a drop of the dispersion was added onto a carbon coated copper grid. The sample was analysed using a JEOL JEM-1011 microscope, operating at 100 kV.

The morphological characterization of MS was also performed by scanning electron microscopy (SEM) with EVO MA10 microscope (Zeiss) at the Center of Microscopy and Microanalysis (UFRGS, Porto Alegre, Brazil). The samples were prepared by dispersing the powder on a carbon conductive tape adhered to the aluminium support, which was then covered with a thin film of gold.

2.10. Laser diffraction analysis

The mean particle size and size distribution (Span) were determined by laser diffraction (Mastersizer®, Malvern Instruments, Malvern, UK) taking into account the particle number (%). The median diameter of each sample (n = 3) was calculated based on the volume-weighted mean diameter (D[4,3]). Each sample was added directly to the dispersion unit (Hydro 2000SM-AWM2002, Malvern, UK) containing 150 mL of distilled water. Measurements were started after reaching an obscuration between 2.8 % and 3.0 %.

2.11. In vitro release profile

The *in vitro* release profile was evaluated using the previously established dialysis bag method (n = 3) in order to evaluate the effect of the RSV or CUR loading in MS on their release rate under sink conditions [36]. Therefore, the release/diffusion/dissolution rate was evaluated for the polyphenols loaded in MS, the polyphenols in solution and their crystalline form in suspension. Briefly, 10 mg of MS-CUR and MS-RSV (corresponding to about 2 mg of each polyphenol) were added to the dialysis bag following by adding of 1 mL of a solution composed of ethanol:water (50:50 v/v). The bags were placed in 250 mL beakers containing 150 mL of the release medium composed of 20 % ethanol, 78 % water and 2 % Tween® 80, to assure the sink conditions during all the experiment. The beakers remained in a water bath at 37 °C under constant stirring for 72 h. Aliquots of 1 mL were collected at predetermined times, replaced by 1 mL of fresh medium and quantified by HPLC, using the method described in section 2.4. Polyphenol solutions were prepared previously by solubilizing 2 mg of pristine CUR or RSV in a 1 ml solution composed of ethanol-water (50:50 v/v) with the aid of ultrasound bath, followed by its adding to the dialysis bag. Finally, for the evaluation of the dissolution rate of the polyphenols crystal forms, 2 mg of RSV or CUR were added to the bag followed by adding 1 ml of a solution composed of ethanol-water (50:50 v/v). The release experiments were carried out for 72 h for all the samples (n = 3), according to the method detailed above.

2.12. Animals

The protocol was approved by the Institutional Ethics Committee of University of Valencia in accordance with current Spanish legislation; and by the regional government in accordance with the guidelines established by the European Union on Animal Care, under protocol code n° 2024-VSC-PEA-0036. For the procedure, Swiss CD1 female mice (4–6 weeks; 25–35 g weight) acquired from Envigo Rms Spain SI (Barcelona, Spain) were used. Animals were stabled in SCSIE facilities (University of Valencia) in separate cages with environmental enrichment (four animals per box). Cages were regularly cleaned and the animals had free access to water and food. The environment had controlled humidity and temperature, as well light and dark cycles every 12 h throughout the livestock stabling and experimental periods. All procedures were conducted in accordance with the ARRIVE guidelines and complied with the U.K. Animals (Scientific Procedures) Act of 1986 and its associated guidelines, the EU Directive 2010/63/EU for animal experiments, and the National Institutes of Health Guide for the Care and Use of Laboratory Animals (NIH Publication No. 8023, revised 1978).

2.13. In vivo DSS induced ulcerative colitis

Animals were randomly assigned to eight experimental groups with five animals per group (n = 6) as described in Table 1, according to the protocol shown in Fig. 1. All groups, except for healthy animals, received DSS diluted into the drinking water (3 % w/v) for 7 days. Animals were euthanised on day 8 by cardiac blood puncture under an optimal anaesthesia protocol with isoflurane. Finally, the entire colon (from the caecum to anus) was resected and divided into portions corresponding to colon anatomy and separated for histological analysis and cytokine level determination.

Table 1
Animal experimental groups and treatments.

Group	Nomenclature	Treatment	Doses
1.	DSS	Non-treated	3 % w/v, v. o
2.	Healthy	Saline (negative control)	0,9 % v/kg, v. o
3.	SULFA	Sulfazalazine (positive control)	100 mg/kg, v. o
4.	MS-CUR	Encapsulated curcumin	200 mg/kg, v. o
5.	MS-RSV	Encapsulated resveratrol	200 mg/kg, v. o
6.	MCM-41	Blank MS particles	200 mg/kg, v. o
7.	CUR	Pristine curcumin	40 mg/kg, v. o
8.	RSV	Pristine resveratrol	40 mg/kg, v. o

DSS = dextran sodium sulphate; SULFA = sulfasalazine; CUR = curcumin; RSV = resveratrol; MS = mesoporous silica; MCM-41 = blank mesoporous silica.

2.14. In vivo efficacy and assessment of colitis

Animal body weight, stool consistency, occurrence of diarrhoea, rectal bleeding and DSS solution volume intake were recorded daily throughout the entire experiment. The Disease Activity Index (DAI) was determined according to Mladenovska et al. assessing weight loss, stool consistency and rectal bleeding [37]. The average calculated from each individual score observation formed the final clinical score ranging from 0 (healthy) to 4 (maximal activity of colitis), as described in Table 2.

Resected colon tissue samples were rinsed with cooled phosphate buffer to remove luminal content. Tissue wet weight and colon length were determined and expressed as a colon weight/length ratio. Then, samples were frozen immediately in liquid nitrogen and stored at −80 °C until further use.

2.15. Inflammatory cytokines detection

The entire colon of each animal (n = 3) was thawed and pulverised in an antiprotease cocktail buffer (10 mM HEPES, 1 mM EDTA, 1 mM EGTA, 10 mM KCl) [38]. Then, the homogenates were centrifuged at 15000 RPM for 15 min, and the supernatant was collected and stored at −80 °C. For enzyme linked immunosorbent assays (ELISA), commercial kits were used to quantify IL-1β, IL-6, TNF-α and IL-4 as inflammatory mediators. Quantification was performed according to the instructions provided by the ELISA kit manufacturer (Thermo Fisher Scientific, Waltham, USA).

2.16. Histological study

Colon samples used for histopathology (n = 3) were opened longitudinally along the main axis, rolled up in a spiral starting from distal to proximal margin and fixed in 4 % formaldehyde. Then, samples were sectioned after being paraffin-embedded and, finally, stained with haematoxylin and eosin. The slides were analysed according to disruptions in the epithelial layer and harm to the mucosa with white cell extravasation (leukocyte infiltration).

2.17. Statistical analysis

Statistical analysis was carried out using Student's t-test in the case of simple comparisons. For multiple comparisons, one-way ANOVA, or one-way ANOVA with repeated measures, followed by post hoc Tukey's test at a 5 % statistical significance level was used (GraphPad Prism software, version 5.00.288 GraphPad Software, Inc., USA).

3. Results and discussion

MS particles have different structures, size and pore arrangements, depending on their synthesis. They usually allow the incorporation of a significant amount of drug, due to their large surface area and pore volume, improving their interaction with aqueous solvents, and optimizing the solubility of poorly water-soluble substances. Herein, the results of the synthesis, characterization and loading of RSV and CUR will be detailed, focused on the ability of the nanometric pore size to reduce molecular crystallization. Furthermore, *in vitro* release studies under sink conditions and the application of the particles in an *in vivo* UC model are presented and discussed.

3.1. MS particles characterization and polyphenols encapsulation

After synthesis of the MS particles and incorporation of the polyphenols CUR or RSV, the samples were characterised in order to verify the porous structure and the incorporation of the polyphenols into their pores. The N_2 adsorption and desorption isotherms (Fig. 2) present a

Table 2
Assessment of disease activity index (DAI) according to Mladenovska et al. [37].

Score	Weight loss	Stool consistency	Rectal bleeding
0	None	Well formed	No blood
1	1–5 %	- -	- -
2	5–10 %	Pasty and semi-formed stools that did not stick to the anus	Positive findings
3	10–20 %	- -	- -
4	>20 %	Liquid stools that stick to the anus	Gross bleeding

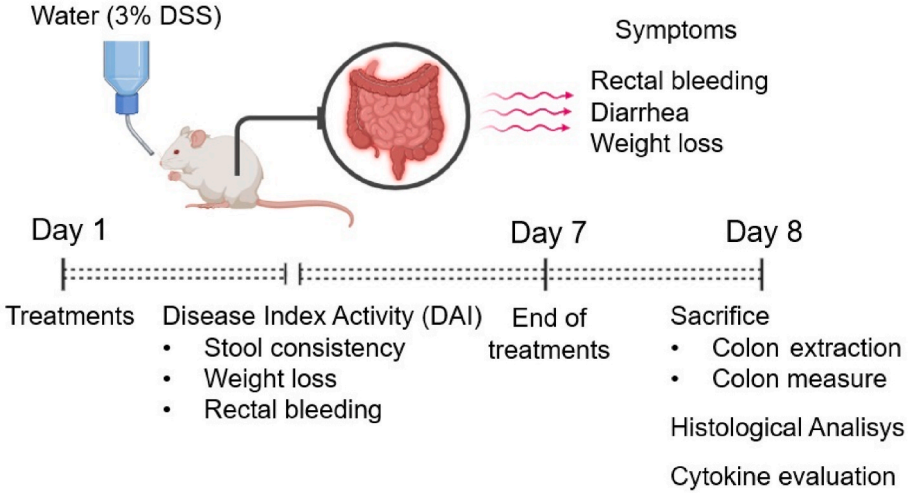

Fig. 1. Experimental design of ulcerative colitis. Illustration created with Biorender.com under an active license.

type IV profile, characteristic of mesoporous materials with pores smaller than 4 nm [39]. The MS particles had a surface area of 875 m^2 g^{-1} and a pore volume of 0.782 cm^3 g^{-1}, in accordance with the values assigned for MCM-41 type particles [40]. After the incorporation of RSV and CUR, it is possible to observe a decrease in the amount of nitrogen adsorbed (Fig. 2-A and 2-C), as well as a decrease in the surface area of MS-RSV (634 m^2 g^{-1}) and MS-CUR (635 m^2 g^{-1}), assigned to the encapsulation of polyphenols. The pore diameter distribution curve (Fig. 2-B and 2-D) obtained by the BJH method, indicates a unimodal distribution, with pores between 2.5 and 3 nm in diameter [41,42]. A decrease in pore volume (0.584 and 0.552 cm^3 g^{-1} for MS-RSV and MS-CUR, respectively) and pore diameter is observed after the incorporation of polyphenols, indicating their presence in MS pores.

The morphology of the MCM-41 (blank MS) structure was investigated in the samples by X-ray diffraction in the range of 1–10° (2θ) and the obtained diffractograms are presented in Fig. 3. The three reflections found in the diffractogram relative to the planes 100, 110 and 200 characterise the hexagonal arrangement of cylindrical pores, which remained unchanged during the polyphenol incorporation process [43,44]. Such cylindrical pores packed in a hexagonal arrangement can be clearly observed in the micrograph obtained by TEM for MS (Fig. 3-B). It is possible to observe a cluster of overlapping particles with pores measuring 2–3 nm, distributed in an orderly manner in parallel channels in a hexagonal arrangement, which corroborates the synthesis process carried out and also the pore diameter and the X-ray diffraction data [45,46]. The high homogeneity of the channels is attributed to the use of an autoclave in the synthesis [47]. Additional TEM analysis determined that the morphology of the developed carrier is not affected by the loading with the drugs (Fig. S1). Moreover, SEM images allowed for the estimation of particle sizes within the submicrometer range, approximately 200–500 nm (Fig. 4A). This observation was corroborated by laser diffraction measurements, which revealed a volume-weighted mean diameter (d4,3) of 343 ± 66 nm for the plain MS (Fig. 4B) with a Span value < 1.5 (n = 3). Similar particle size ranges were observed for the MS-RSV and MS-CUR formulations, with mean diameters (d4,3) of 437 ± 78 nm and 254 ± 10 nm, respectively, as shown in Fig. S2.

The polyphenol incorporation into the MS pores was carried out using the incipient wetness method and the effective amount incorporated was determined by HPLC. The analytical determination proved to be linear, with correlation coefficients (r^2) of 0.9995 for RSV and 0.9999 for CUR, in the concentration range from 2.5 to 25 μg mL^{-1}. Furthermore, the methods were validated for precision, accuracy, and specificity. The determined limits of detection for RSV and CUR were 0.29 and 0.14 μg mL^{-1}, respectively; while the limits of quantification were 0.87 and 0.43 μg mL^{-1} respectively for RSV and CUR. The polyphenol content values obtained for MS-RSV and MS-CUR indicated recoveries of 95 ± 1.2 % and 90 ± 2.1 %, respectively. The drug loading (DL) determined after extraction of polyphenols from MS was 18.4 % for RSV, and 17.4 % for CUR. These results are in accordance with the calculated theoretical loading of 19.35 %.

DL of the polyphenols was also evaluated by thermogravimetric analysis. The thermograms (Fig. 5-A and 5-B), showed a mass loss from 300 °C for RSV and CUR, culminating in a complete degradation around 650 °C. This degradation temperature range (300–650 °C), was also observed in the MS-RSV and MS-CUR thermograms, indicating an organic content of 19.6 % for MS-CUR and 17.7 % for MS-RSV, thus corroborating the results obtained using the HPLC analysis.

MS carriers possess the ability to internalise molecules within their nanometer-sized pores by capillary forces, a process that has been linked

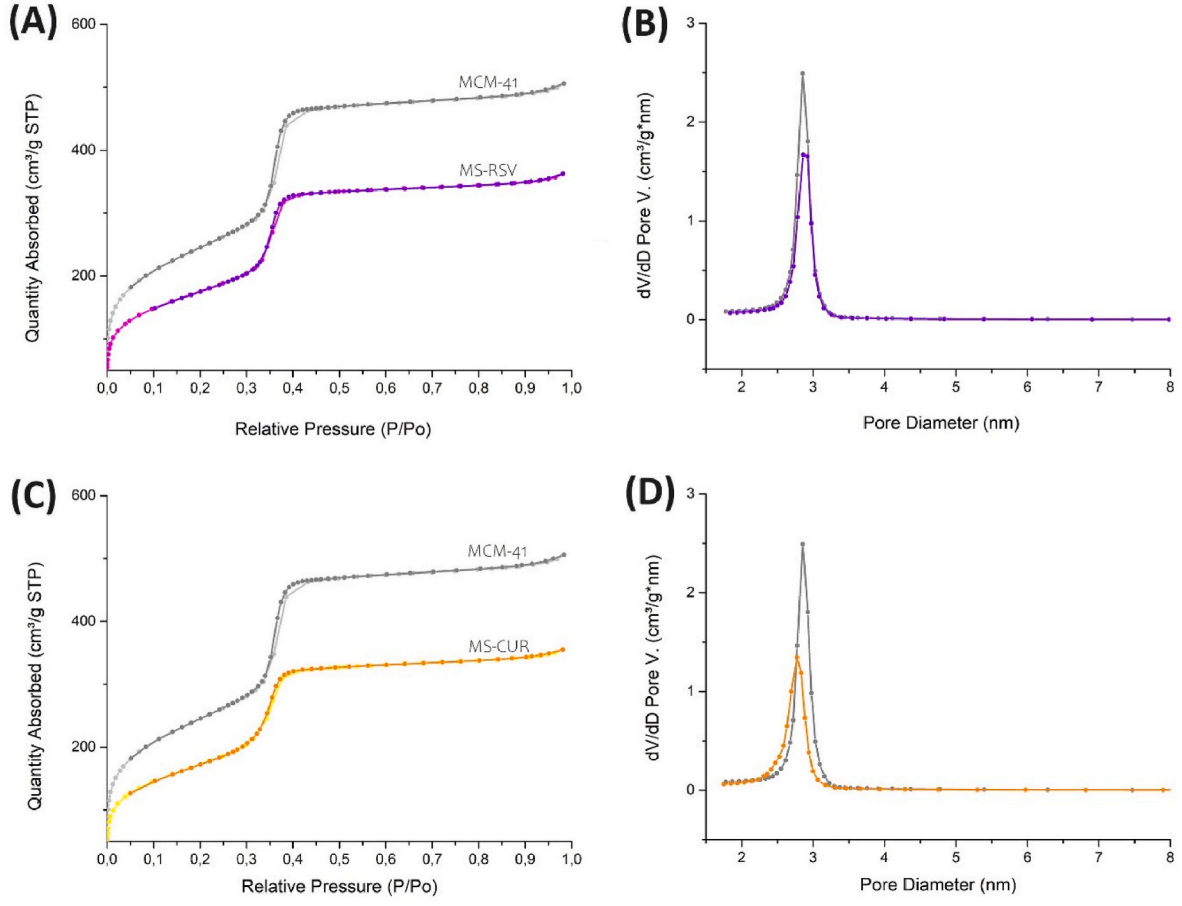

Fig. 2. Nitrogen adsorption-desorption isotherms and pore size distribution for MS (MCM-41) in comparison with MS-RSV (**A** and **B**) and MS-CUR (**C** and **D**).

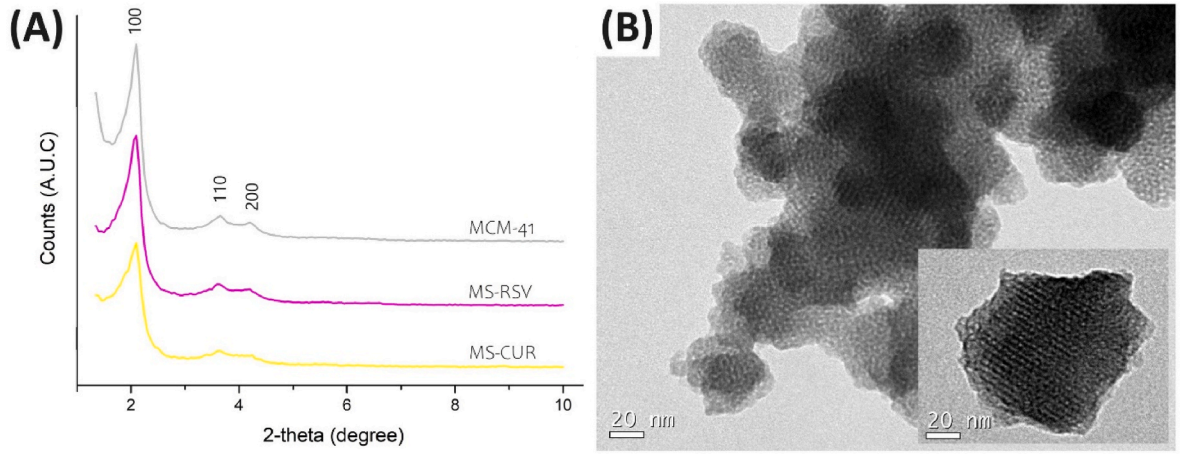

Fig. 3. **A**) XRPD diffractograms in the range of 2θ = 1–10°; **B**) TEM images of MS particles.

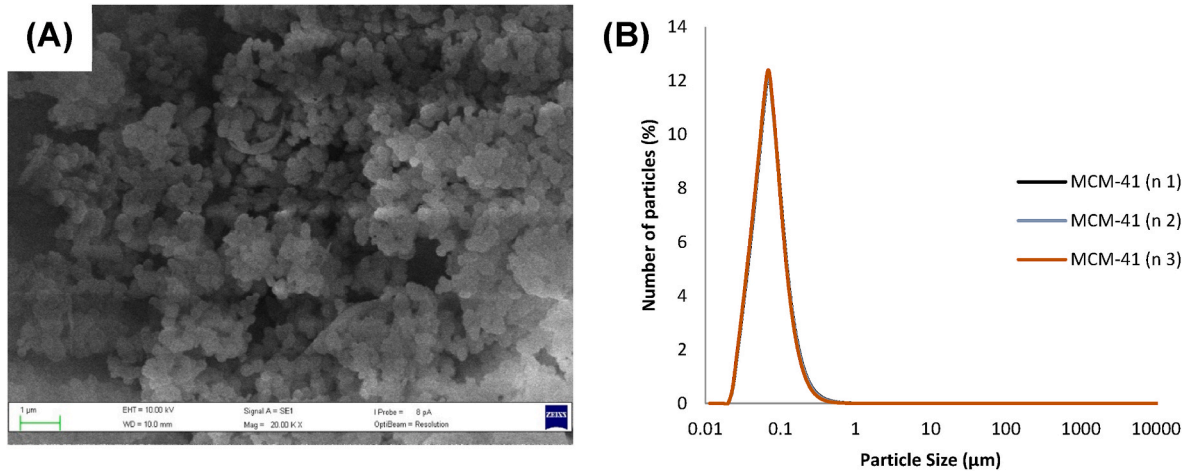

Fig. 4. **A**) SEM analysis of the MS particles; **B**) Laser diffraction analysis of the MS particles (n = 3).

to the formation of encapsulated active ingredients in an amorphous state due to a physical confinement effect [48]. To explore this phenomenon, solid-state characterisations were conducted, and the resulting DSC curves are presented in Fig. 5-C and 5-D.

The DSC curve of RSV (Fig. 5-C) showed the presence of an endothermic peak at 263 °C, corresponding to the melting point of the polyphenol in the crystalline state [49]. In the MS-RSV sample, the presence of this endothermic peak was not observed, demonstrating that the molecules were in a non-crystalline form [50]. However, this endothermic peak was also not shown with the PxM RSV, so a conclusion could not be made regarding the physical state of this polyphenol. One hypothesis is that partial or total amorphization of the PxM was induced by the heating process during the DSC analysis (300 °C), and the polyphenol could melt, resulting in an interaction with silanol groups present on the surface of the silica particles [51].

In the case of CUR (Fig. 5-D), a similar pattern is observed, where an endothermic peak, related to the melting point of CUR in the crystalline state (177 °C), can be identified [52]. However, it is important to note that this endothermic peak is subtly present in the MS-CUR curves and the respective physical mixture (PxM CUR), with reduced intensity. This similar DSC pattern as for RSV also suggests a non-crystalline state of the polyphenol when combined with MS [53]. The broad signals in the curves below 100 °C were attributed to the presence of water. The possible amorphous condition conferred by encapsulation in MS was further evaluated by X-ray diffraction analyses.

The XRDP diffractograms of all components are shown in Fig. 6. The MCM-41 curve displays only the amorphous silica halo at 2θ *ca.* 23°, which is also observed in the other samples containing MS. Nonetheless, the diffraction profile obtained for MS-RSV (Fig. 6-A) revealed the absence of some reflections, identified with red marks in pristine RSV and PxM RSV. Even so, most of the reflections were located in the same positions as those observed for the polyphenol, but at lower intensity.

The diffractograms of MS-CUR (Fig. 6-B), showed a similar behaviour to MS-RSV. MS-CUR also exhibited some absent reflections marked in red, but most of the same characteristic reflections of the crystalline profile of pristine CUR and the PxM CUR were observed, with considerably less intensity. These results suggest the occurrence of a crystalline arrangement of the polyphenols partially converted to their amorphous form when encapsulated in MS [54]. This partial amorphization is related to the increased solubility of poorly water-soluble drugs, since the molecules arrangement inside of the pores can improve their interactions with water [55].

FTIR analyses were conducted in order to identify potential interactions between functional groups of MS and polyphenols (Fig. S3, supplementary material), and also to evaluate the CTAB removal after the calcination process during synthesis. MCM-41 indicates bands from silica (SiO_2) at 1200 to 1000 cm^{-1}, with a maximum at 1080 cm^{-1}, corresponding to Si-O stretching. The band at 960 cm^{-1} is due to Si-OH stretching, assigned to the presence of remaining silanol groups. Si-O-Si bonding can also be seen at 810 cm^{-1} [56]. The presence of a broad band in the range of 3200–3400 cm^{-1} is related to the O-H band of hydroxyls from the silanol groups of silica and also from adsorbed water [57,58].

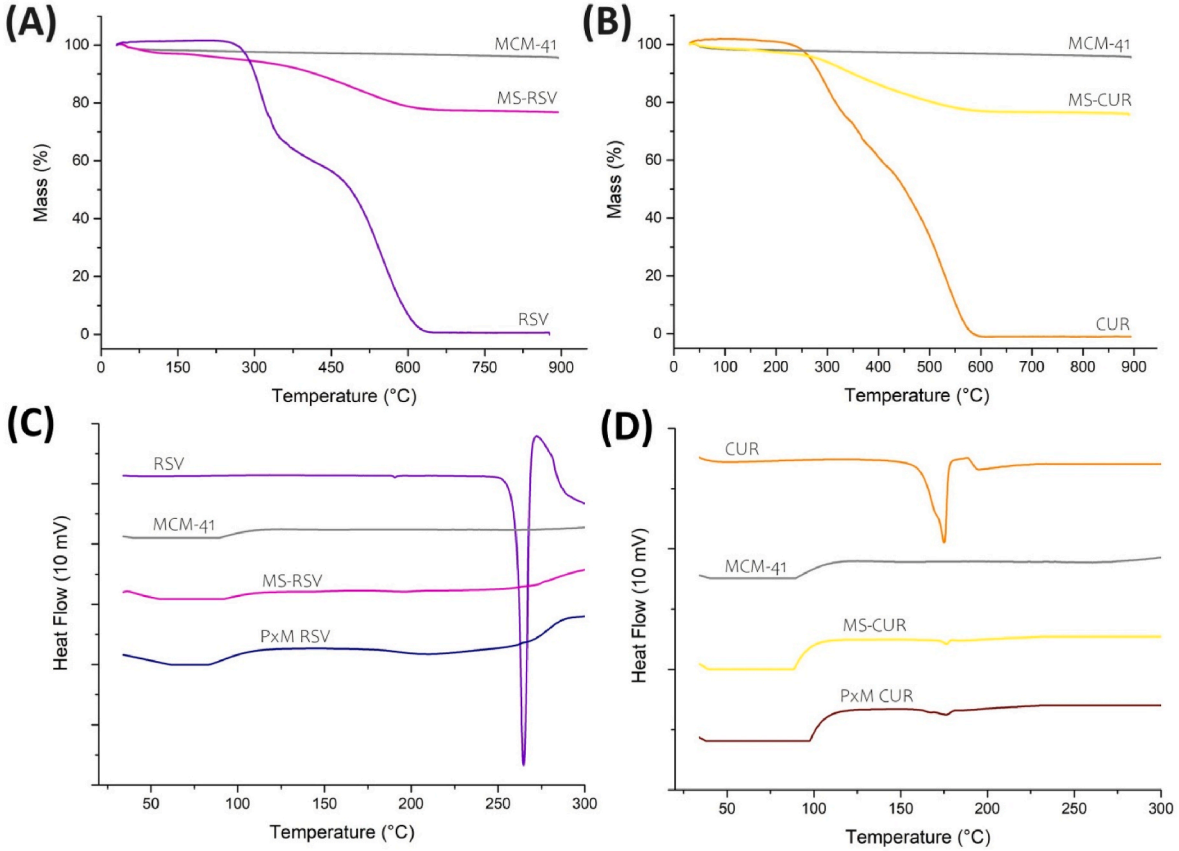

Fig. 5. Thermal analysis. **A**) TGA of MS-RSV and constituents; **B**) TGA of MS-CUR and constituents; C) DSC of MS-RSV and constituents; D) DSC of MS-CUR and constituents.

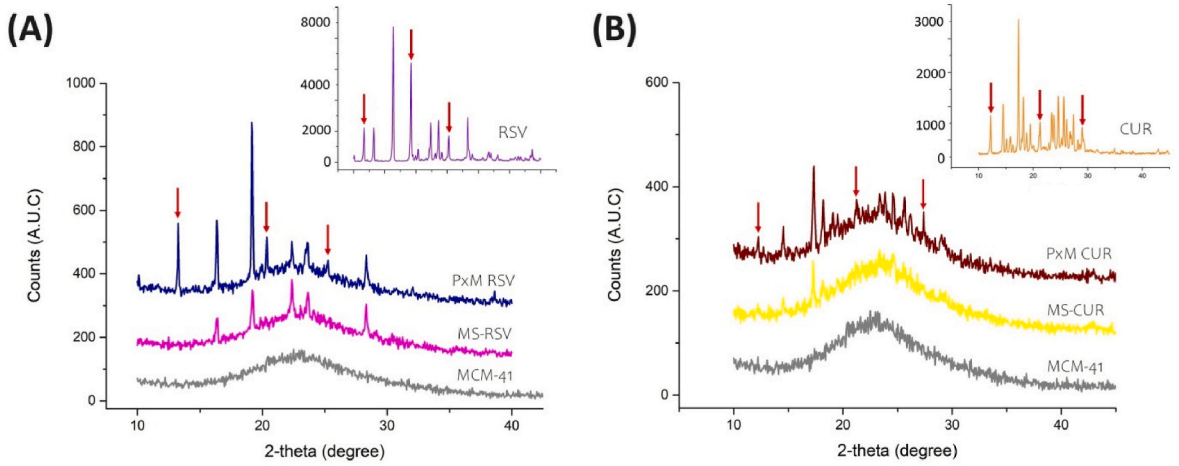

Fig. 6. XRDP analysis. **A**) RSV diffractograms and constituents; **B**) CUR diffractograms and constituents.

Herein, the absence of other bands showed a complete calcination process in the syntheses by total removal of the surfactant. MS-CUR and MS-RSV samples showed bands at 1500 to 1610 cm^{-1}, similar to the ones of pristine polyphenols, which are related to the presence of phenolic rings in their chemical structures, denoting successful incorporation of the active ingredients in MS, but without significant intermolecular interactions [59,60].

3.2. *In vitro* release studies

In vitro release studies are commonly used to demonstrate differences or similarities between formulations around a main substance under sink conditions, mainly for poorly soluble substances, like RSV and CUR. Herein, the studies were performed using the dialysis bag method. The dissolution/diffusion profiles of MS-RSV and MS-CUR were compared with the free polyphenols (soluble in a mixture of ethanol and water, 50:50) and the pristine polyphenols (crystalline form) (Fig. 7).

RSV and CUR in their free forms (organic solution) underwent complete diffusion (100 %) in 4 and 36 h, respectively, while MS-RSV and MS-CUR reached 39 ± 5.4 % and 15 ± 0.2 %, in these respective periods, demonstrating a statistically significant difference for both formulations ($p < 0.001$). Furthermore, MS-RSV showed a 100 %

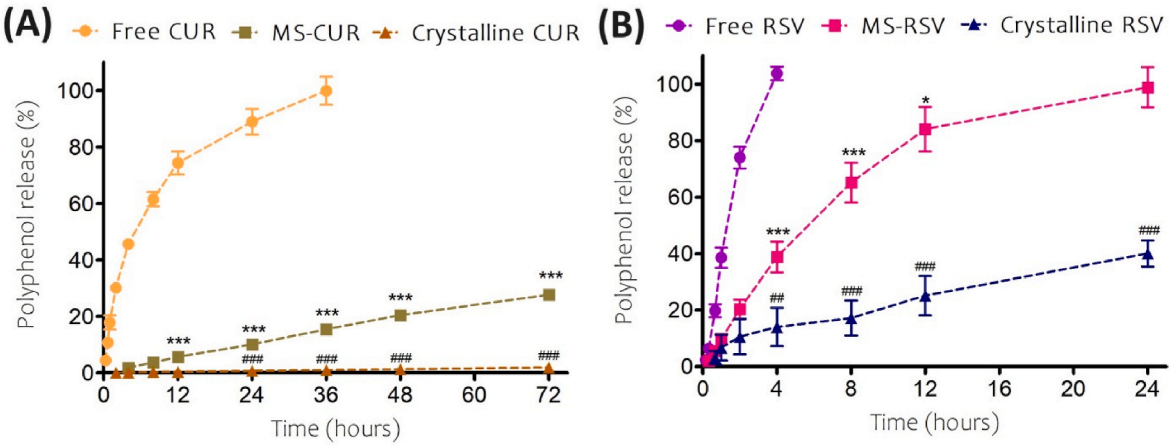

Fig. 7. *In vitro* release profiles. **A**) CUR forms; **B**) RSV forms. Unpaired Student's t-test of free polyphenols compared to MS-CUR/RSV. *p < 0.05; **p < 0.01; ***p < 0.001. Unpaired Student's t-test of crystalline polyphenols compared to MS-CUR/RSV. ##p < 0.01; ###p < 0.001.

polyphenol release after 24 h, and MS-CUR reached 28 ± 1.3 % at the end of 72 h, indicating a sustained release profile. The incorporation of polyphenols into MS particles enabled a gradual and controlled release, this feature being an interesting property for the development of pharmaceutical formulations, as it ensures the most effective delivery of the active ingredient [61,62], without a burst of release that could lead to toxicity problems or decreased drug bioavailability.

Moreover, to evaluate the increase in the apparent solubility of the polyphenols by means of their incorporation into MS particles, it was fundamental to compare their release data from MS with those obtained for both polyphenols in their crystalline state. As shown in Fig. 7, at the end of 72 h, crystalline CUR reached 2 ± 0.6 %, while crystalline RSV achieved 40 ± 4.6 % in 24 h, showing a statistical difference compared with MS-CUR and MS-RSV, respectively. For non-soluble substances, a slower and more limited release rate is expected, particularly with these polyphenols [63,64].

The release rate of substances incorporated into mesoporous particles is influenced by several factors, including pore size, channel arrangement [65], DL content, and molecular packing density [66]. Pore size plays a critical role in governing molecular diffusion and solvent ingress; larger pores generally increase diffusion rates [67]. Additionally, the hydrophobicity of the incorporated molecules significantly affects release behaviour; more hydrophobic active compounds tend to exhibit slower release rates due to their reduced interaction with the surrounding medium [68]. These differences reinforce the ability of the MS particles to improve water solubility t due to their partial amorphization as discussed before, along with the large surface area of MS particles enhancing the dispersion of molecules, promoting by increased wettability. Thus, the behaviour of the incorporated polyphenols offers a promising alternative for the treatment of UC.

In the context of oral administration, the gastrointestinal tract presents several barriers, the most notable being the variation in pH levels and the presence of digestive enzymes. Both CUR and RSV exhibit good stability under acidic conditions up to pH 8, which extends throughout the gastrointestinal tract. However, CUR is slightly less stable compared to RSV [69,70]. Some studies have evaluated the release profiles of both RSV and CUR under pH conditions that mimic those of the gastrointestinal tract [32,59,71]. Pujara and collaborators [72], conducted a study using both free CUR and CUR conjugated with β-lactoglobulin, evaluating their release profiles under gastrointestinal pH conditions (pH 1.2, pH 5.0, and pH 7.4), in the presence and absence of digestive enzymes. The results showed that the pH conditions had a significant influence on the release rate of curcumin from the different formulations, but free curcumin showed only 5.5 % release throughout the experiment, with only slight influence by the pH conditions. Gao and colleagues investigated the release profile of CUR incorporated into mesoporous silica microspheres under various pH conditions (pH 1.2, pH 6.8, and pH 7.4) [33]. The results demonstrated slight differences of CUR release rate at different gastrointestinal pH values. Similarly, Yang and collaborators [16] evaluated the release profile of CUR incorporated into mesoporous silica nanorods at pH 5.0 and pH 7.4, demonstrating that pH did not significantly affect the release rate of CUR from the mesoporous silica formulations. In our study, the primary objective was to assess the ability of mesoporous silica (MS) to control the release rates of CUR and RSV, in comparison with their respective solutions and crystalline forms (as suspensions). Therefore, release experiments were conducted under sink conditions without monitoring the apparent pH of the medium, since the release medium was an organic solvent.

Nevertheless, we are planning future studies to investigate the release behaviour of CUR and RSV from our formulations in biomimetic media at different pH values. These studies will provide deeper insights into *in vitro–in vivo* correlations and will enable the application of pharmacometrics analyses.

3.3. *In vivo ulcerative colitis induction*

UC is a chronic, persistent disease that leads to various complications, including weight loss, bleeding, increased susceptibility to intestinal infections, abdominal pain, and flatulence, among others. These symptoms significantly disrupt the daily routines of those affected, ultimately reducing their quality of life in a significant way. These symptoms were evaluated and scored to determine the severity of the UC state. Herein, during the induction of the UC by DSS intake in mice, their symptoms were assessed over a 7-day treatment throughout the period using the DAI scoring system. The results are shown in Fig. 8. Moreover, weight loss is reported in Table S1 in the supplementary material section.

The DAI evaluation revealed significant differences between the Healthy and DSS control groups ($p < 0.001$). DSS intake for 7 days caused moderate weight loss, moderate-to-severe bleeding, and liquid stool. A significant difference was also observed between the DSS and SULFA groups ($p < 0.01$), indicating remission of symptoms in the SULFA-positive control group, even though some of the UC symptomatology was also observed. For formulations containing CUR, the MS-CUR treatment group exhibited an important symptom remission compared with the DSS group until day 6 ($p < 0.001$), a result not observed with the non-encapsulated drug (CUR). However, no significant difference between MS-CUR and CUR was found at 7 days. This could be caused due to the increase of harmful DSS effects after long-term administration.

Regarding formulations containing RSV, both MS-RSV and pristine RSV showed significant differences compared with the DSS group ($p <$

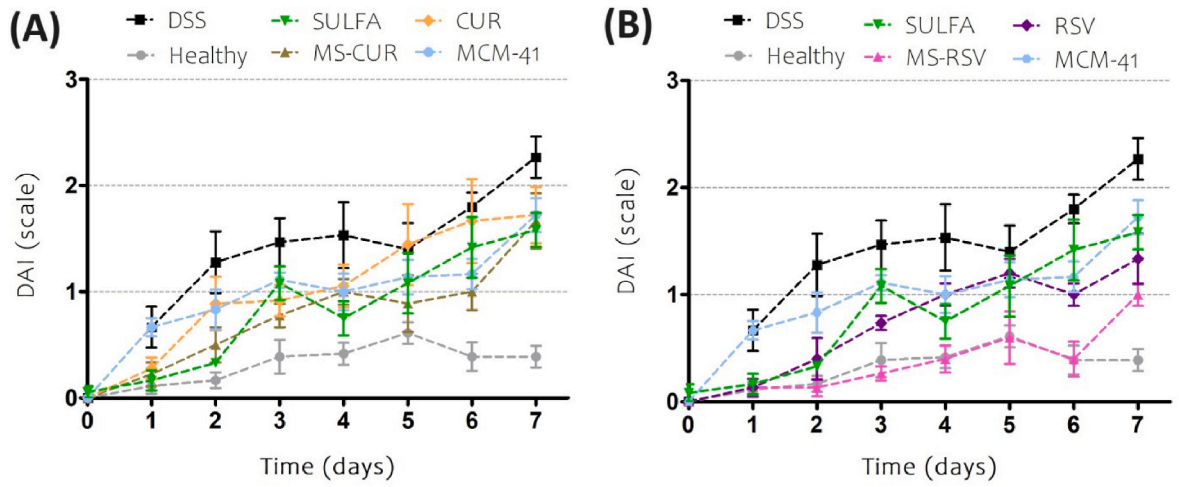

Fig. 8. Disease Activity Index. **A**) CUR treatments; **B**) RSV treatments. Healthy = (saline 0.9 %) negative control; DSS = disease control; SULFA = sulfasalazine (100 mg/kg) positive control; MCM-41 = blank MS particles (200 mg/kg); CUR = curcumin (40 mg/kg); MS-CUR = curcumin loaded MS particles (200 mg/kg); RSV = resveratrol (40 mg/kg); MS-RSV = resveratrol loaded MS particles (200 mg/kg) (One-way ANOVA, with repeated measures, post hoc Tuckey's test).

0.001) however no differences between them were found. Nevertheless, MS-RSV was the only group to show a difference from the SULFA-positive control ($p < 0.01$), suggesting better pharmacological performance, thanks to the silica particles. The administration of blank MS particles (MCM-41) did not show significant differences in comparison to the DSS group ($p > 0.05$), indicating that the presence of active substances was a decisive factor in the DAI assessment.

Symptom assessment is a key parameter for evaluating the quality of life of UC patients, since symptom remission is directly associated with an improved quality of life. The use of DSS at concentrations ranging from 2 % to 5 % has been widely used to induce an UC-like condition, offering a relatively simple and cost-effective *in vivo* model of the disease [73]. Yao et al. [74] induced UC in BALB/c mice (18–20 g) using 5 % DSS over 7 days, followed by treatment with two doses of RSV (30 and 60 mg/kg). Both doses showed a statistically significant difference from DSS starting on day 5. However, RSV was solubilised in 200 μL of ethanol before adding the vehicle, a process that may enhance drug absorption. Clinical studies in UC patients using RSV at doses of 500 mg/day demonstrated a reduction in symptoms and improvements in both quality of life and patient well-being [75,76]. These findings support the potential of RSV as an adjuvant treatment option forUC. The use of MS particles also presented support for the use of solvent-free formulations.

CUR has been extensively studied, with different nano-based pharmaceutical technologies, such as liposomes and micelles, being employed to enhance its solubility, absorption, and permeability [77,78]. Wei et al. conducted a study inducing UC in BALB/c mice (22–26 g) using 5 % DSS, followed by the administration of CUR (100 mg/kg/day) for 7 days [79]. The DAI results indicated symptom remission in the CUR-treated group compared with the DSS group. However, CUR was pre-solubilised in 200 μL of a 5 % ethanol solution similarly to the Yao et al. study. Another similar study administered CUR in different doses (15, 30, and 60 mg/kg, intraperitoneally), leading to a significant reduction in DAI values and symptom remission. Likewise, the vehicle used in this study contained ethanol (2.5 %) [80]. Clinical studies have also investigated the use of CUR in combination with mesalazine, showing a significant reduction in DAI scores in UC patients compared with placebo groups [81,82]. However, a study administering CUR alone (150 mg, 3x/day) did not show any significant differences with the non-treated condition [83]. The results observed in these studies align with the outcomes of the current research.

UC induced inflammation often leads to a shortening of the colon. Therefore, colon length measurement is an important indicator of UC severity, since it is associated with improvements of the symptoms in this method and since pharmacological treatments should aim to partially or fully reverse it [73]. Fig. 9 summarises the colon length and colon weight-to-length ratio measurement data.

The colon length (Fig. 9-A) in the DSS (6.3 ± 1.3 cm) control group showed significant shortening in comparison to the Healthy group (9.3 ± 1.1 cm) ($p < 0.01$), confirming the validity of the induction method. However, the positive control SULFA (6.4 ± 0.5 cm) did not reverse the length decrease, showing also a significant difference compared with the Healthy control ($p < 0.01$). This could be explained by possible adverse effects commonly associated with prolonged treatment with sulfasalazine [7], or an inability to achieve full action or protection. Among the polyphenol treatments, pristine CUR (6.7 ± 1.3 cm) was the only group that showed a colon shortening with respect to the Healthy control ($p < 0.05$). This result highlights the potential of MS particles to enhance the bioavailability of CUR. Although pristine RSV (7.6 ± 0.6 cm), MS-CUR (8.1 ± 0.2 cm) and MS-RSV (7.8 ± 0.4 cm) treatments did not show significant differences compared to the DSS group, they also did not differ from the Healthy group, suggesting the existence of a pharmacological action against the disease and similarity in their effects. The MCM-41 particles (6.7 ± 1.1 cm) showed a significant difference from the Healthy group ($p < 0.01$), indicating that without polyphenol encapsulation, the MS particles do not have pharmacological effects.

UC inflammation is commonly associated with the development of oedema, which becomes more pronounced under pathological conditions such as UC [81]. Regarding the colon weight-to-length ratio (Fig. 9-B), higher values were observed for the DSS, SULFA ($p < 0.01$), and MCM-41 ($p < 0.05$) groups compared with the Healthy control. Among the formulations tested, MS-CUR was the only one to show a statistically significant difference compared to the DSS control ($p < 0.05$), suggesting an anti-inflammatory effect in this treatment group. In the same way as for the colon length observations, the other treatments, despite showing no difference compared to the DSS group, also did not appear to be significantly different from the Healthy group, which may indicate a similar trend of effects on disease progression.

Several studies involving these polyphenols have focused on the observation of the recovery of colon size using UC induction models with DSS [84–87]. Many polyphenols act as antioxidants by neutralizing cell-derived by-products, such as reactive oxygen species, which can damage the mucosa and hinder recovery [88,89]. Beyond this well-established pharmacological action, the metabolites of RSV and CUR support gut microbiota by serving as substrates for the restoration of normal flora. This, in turn, enhances the symbiotic relationship with

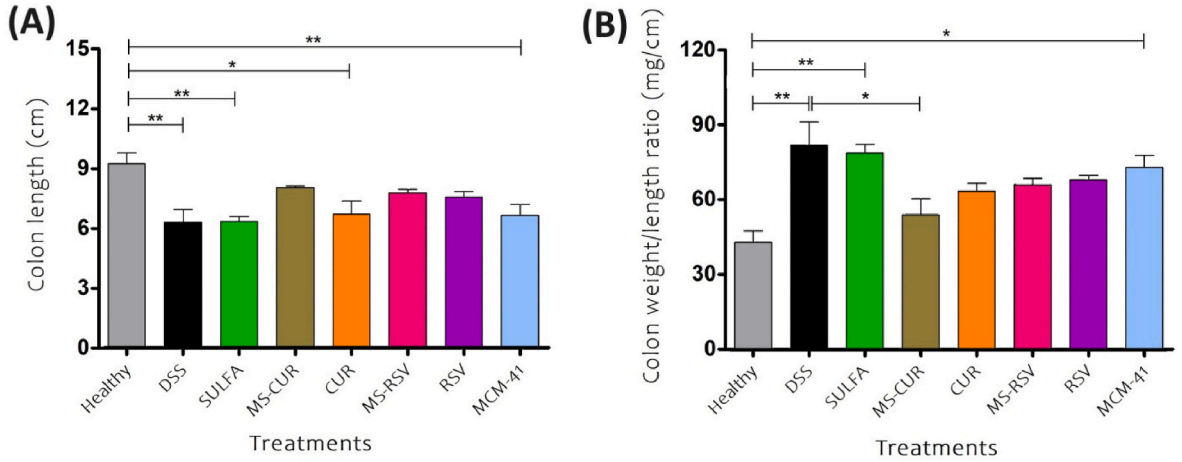

Fig. 9. **A**) Colon length; **B**) colon weight-to-length ratio. Animal groups: Healthy = (saline 0.9 %) negative control; DSS = disease control; SULFA = sulfasalazine (100 mg/kg) positive control; MCM-41 = blank MS particles (200 mg/kg); CUR = curcumin (40 mg/kg); MS-CUR = curcumin loaded MS particles (200 mg/kg); RSV = resveratrol (40 mg/kg); MS-RSV = resveratrol loaded MS particles (200 mg/kg) (One-way ANOVA, post hoc Tuckey's test; *p < 0.05; **p < 0.01).

the mucosa and promotes the proliferation of beneficial microorganisms in the intestine [90–93]. These findings align with the results obtained in the colon measurement experiments in this study, clearly supporting their potential therapeutic effects.

MS particles are inert to the organism; however, their small size, covering population distributions from 200 nm to 10 μm, may facilitate their accumulation in intestinal villi by fenestration [94]. One clinical trial tested MS particles with pore sizes of 7–12 nm, administered orally to healthy individuals for 21 days and to obese individuals for 10 weeks. The estimated dose was 3 g of MS, taken three times a day. Blood, faeces, urine, and potential adverse effects were monitored throughout the study. By the end of the experiment, participants reported mild abdominal discomfort, such as flatulence, and minor changes in intestinal motility. Renal function remained stable, with no changes in creatinine levels, and ortho-silicic acid was detected in the urine, confirming particle degradation. Overall, the administration of 9 g of MS particles per day was deemed safe [27]. Tam et al. assessed the adhesion capacity of silica particles containing a fluorescent marker in an animal

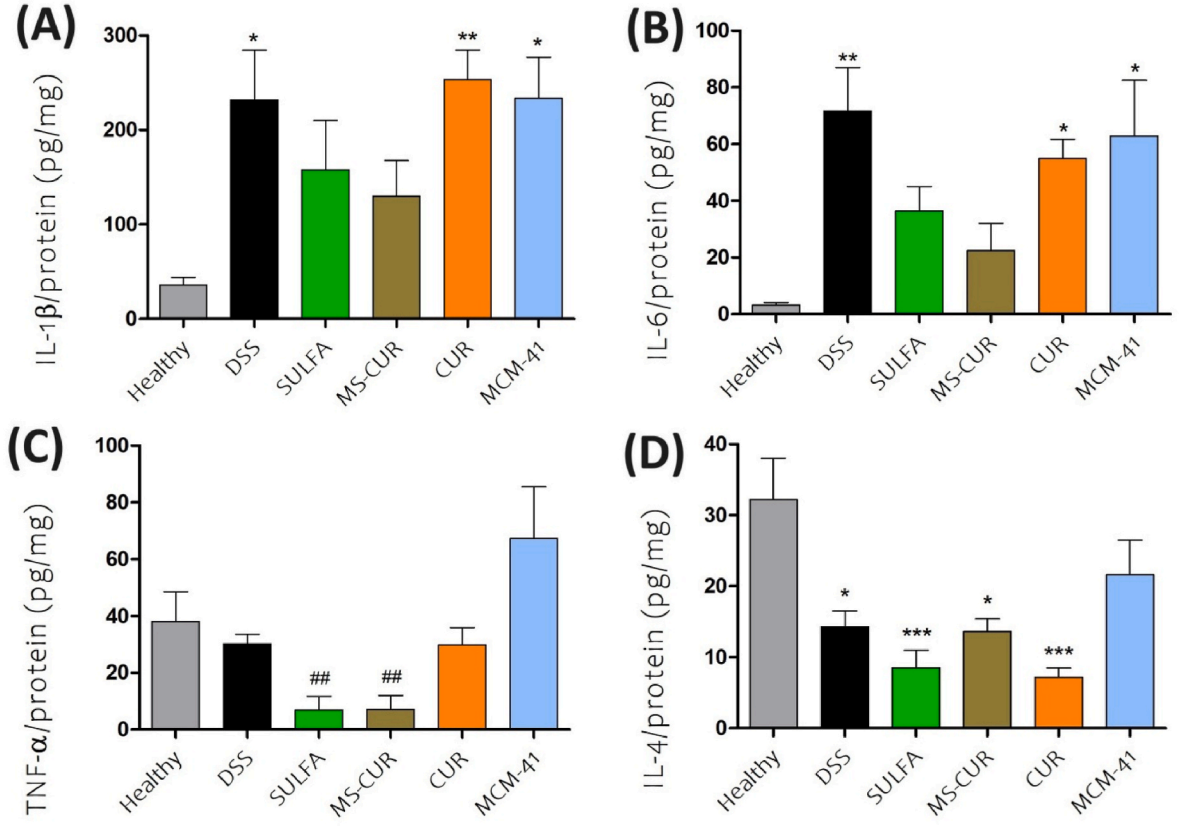

Fig. 10. Cytokine levels evaluation for CUR formulations. **A**) IL-1β; **B**) IL-6; C) TNF-α; **D**) IL-4. Treatments: Healthy = (saline 0.9 %) negative control; DSS = disease control; SULFA = sulfasalazine (100 mg/kg) positive control; MCM-41 = blank MS particles (200 mg/kg); CUR = curcumin (40 mg/kg); MS-CUR = curcumin loaded MS particles (200 mg/kg) (One-way ANOVA, post hoc Tuckey's test; data comparison with Healthy group: *p < 0.05; **p < 0.01; ***p < 0.001; data comparison with MCM-41 group: ##p < 0.01).

model of UC using confocal microscopy [95]. Their results showed that inflammation in the colon enhances the deposition of particles in the affected area up to 24 h after oral administration, facilitating the subsequent release of the particulate drug. In another study, Teruel et al. investigated MS particles loaded with hydrocortisone in rats with inflammatory bowel disease [96]. After oral administration, the particles effectively adhered to the site of action, with no significant drug levels detected in the plasma. Upon dissection, visual improvements in the inflamed tissue were observed.

Inflammatory diseases involve the active participation of the immune system. In the gut, neutrophils, macrophages (differentiated monocytes), and dendritic cells play key roles, releasing a variety of inflammatory cytokines to mediate the inflammatory response [79]. Herein, Fig. 10 demonstrates the results for CUR formulations and the levels of pro-inflammatory cytokines IL-1β, IL-6, TNF-α, and anti-inflammatory IL-4, present in the colon homogenates.

The presence of the pro-inflammatory cytokines IL-1β, IL-6, and TNF-α reflects the severity of inflammation in the colon. Therefore, a reduction in these cytokines may indicate better inflammation control [97]. In contrast, IL-4 has anti-inflammatory properties that help mitigate the harmful effects of inflammation, and its levels are expected to be naturally higher during inflammatory conditions to counterbalance the inflammatory response [98]. The differences observed between the DSS and Healthy control groups once again confirmed the effectiveness of the induced colitis model, at least for IL-1β, IL-6 and IL-4. Among the CUR formulations, pristine CUR showed a significant difference for IL-1β and IL-6 compared with the Healthy control ($p < 0.01$ and $p < 0.05$, respectively), indicating that MS-CUR exhibited an inhibitory effect on IL-1β and IL-6, which are highly pro-inflammatory cytokines [99].

Treatments with both pristine RSV and MS-RSV showed significantly lower cytokine levels (Fig. 11) compared with the DSS group for IL-1β ($p < 0.05$ and $p < 0.01$, respectively) and IL-6 ($p < 0.01$ and $p < 0.05$, respectively). While the inhibitory effect on these interleukins was expected [74,100], the use of MS particles did not show a significant difference when compared to the non-encapsulated RSV.

The presence of cytokines IL-1β, IL-6, and TNF-α is associated with dendritic cells located in the lamina propria of the intestine, just beneath the epithelial layer. An imbalance in these immune proteins increases intestinal permeability by widening the spaces between tight junctions. These inflammatory conditions also contribute to other effects, such as cell adhesion and altered ion transport, this being directly related to diarrhoea. Neutrophils and macrophages release inflammatory mediators like myeloperoxidase (MPO), but they also promote the release of the anti-inflammatory cytokine IL-4 [18]. The reduction in TNF-α levels for both polyphenols was expected [21,80]; however, TNF-α was the only interleukin that did not show a significant difference in the DSS group across these treatments.

The results involving IL-4 showed the absence of its upregulation by any polyphenol-based treatment, with respect to the Healthy group. Anti-inflammatory cytokines, such as IL-4 and IL-10, are considered delayed-acting cytokines because they are typically activated following acute inflammation [101]. As a result, their presence is more prominent in chronic conditions, where they help regulate and reduce prolonged inflammatory responses. Although IL-4 evaluation is very common among inflammatory assays, few studies have investigated the presence or absence of IL-4 in the pathological context of UC [102]. Hoving et al. evaluated the expression of IL-4 and confirmed its presence in UC; however, the colitis induction method in their study used oxazolone

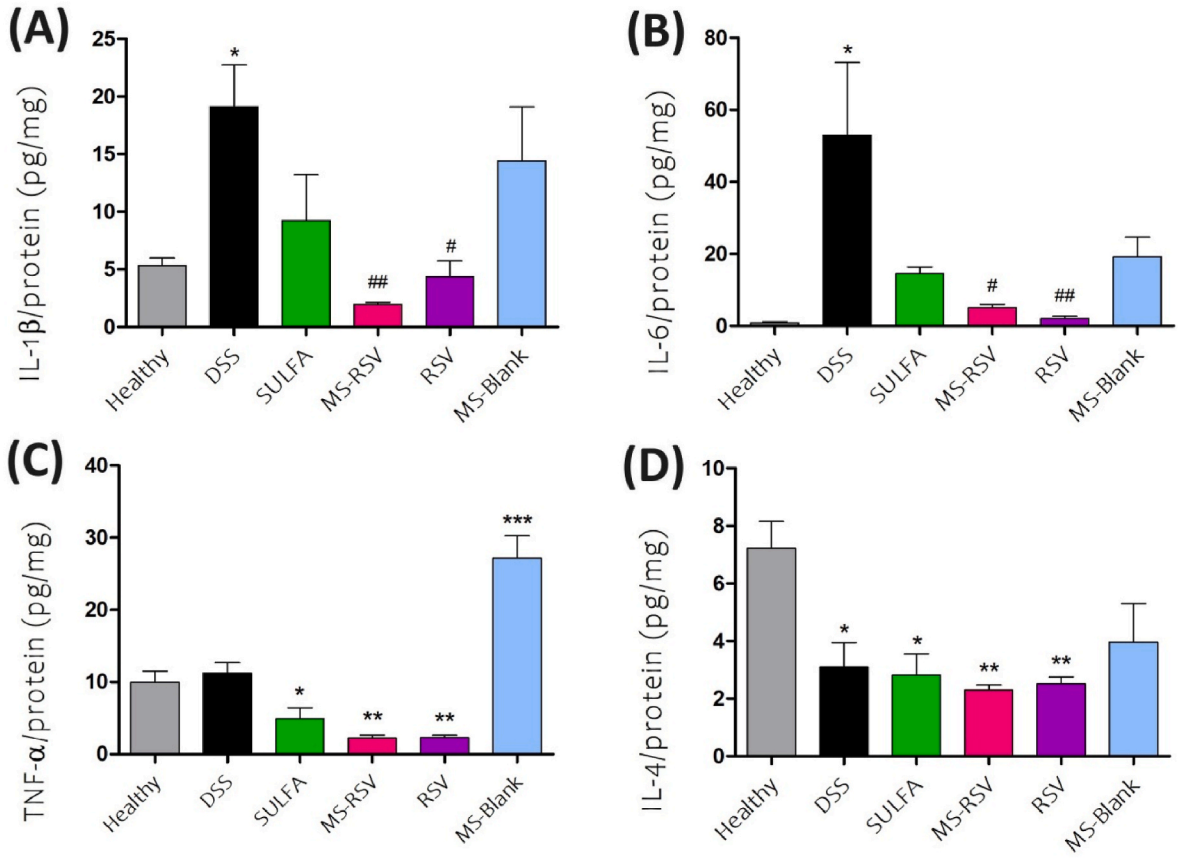

Fig. 11. Cytokine levels evaluation for RSV formulations. **A**) IL-1β; **B**) IL-6; **C**) TNF-α; **D**) IL-4. Treatments: Healthy = (saline 0.9 %) negative control; DSS = disease control; SULFA = sulfasalazine (100 mg/kg) positive control; MCM-41 = blank MS particles (200 mg/kg); RSV = resveratrol (40 mg/kg); MS-RSV = resveratrol loaded MS particles (200 mg/kg) (One-way ANOVA, post hoc Tuckey's test; data comparison with Healthy group: *$p < 0.05$; **$p < 0.01$; ***$p < 0.001$; data comparison with DSS group: #$p < 0.05$; ##$p < 0.01$).

[98]. Heller et al. evaluated IL-4 expression mediated by Th2 cells *in vitro*, using colonic lamina propria muscle cells [103]. Their results indicated the absence of IL-4 production in an environment simulating induced inflammation.

Inflammatory conditions in the colon disrupt mucus production by goblet cells, weakening the tissue's natural defences and triggering a series of inflammation-related events. Alongside dysplasia in the epithelial tissue, immune cell migration intensifies the reactivity of the process, potentially causing damage to the cellular matrix, increased collagen deposition, and fibrous formations in the lamina propria where most immune activity occurs. Ultimately, colon injuries can lead to atrophy of colonic crypts, which are located between the intestinal villi and are responsible for secreting enzymes that regulate the pH of the area [86,99]. In this study, histological sections were obtained from the animals following the UC induction experiment, and the results are presented in Fig. 12.

From the histopathological point of view, DSS-induced UC is mainly characterised by, on the one side, fibrosis in mucosa and submucosa, and on the other side, infiltration of granulocytes, lymphocytes and macrophages [104]. The histopathological assessment was in agreement with previous findings [105]. After DSS intake (Fig. 12-B) severe tissue damage was observed, specifically mucosal tissue degeneration and leukocyte infiltration. These histopathological signs were less marked in the polyphenol-treated animals: CUR, RSV, MS-CUR and MS-RSV, indicating that these formulations can exert against inflammation damage to intestinal tissue. However, it should be noted that, though CUR and RSV (Fig. 12-E and 12-G) diminished the presence of white cell extravasation into intestinal tissue, MS-loaded formulations (Fig. 12-D and 12-F) showed an even lower cell infiltration, which suggests again that MS improves the bioavailability of the drugs and subsequently enhances their pharmacological activity. As expected, unloaded MCM-41 (Fig. 12-H) presented considerable inflammatory infiltration and mucosal tissue degeneration, confirming that unloaded MS does not have a pharmaceutical effect.

Oral administration is the simplest and most practical route for drug administration; however, natural barriers such as pH, enzymes, and absorption processes reduce the bioavailability of many compounds, making it challenging for drugs to achieve their full therapeutic potential [106]. In the case of UC, the reduced mucus production and the inflammatory environment, which increases local permeability, may facilitate drug absorption [107]. However, the goal in UC treatment is to target the intestinal tissue locally, rather than systemically. Silica particles, as demonstrated in previous studies [27,96], can alter intestinal motility due to particle deposition in the tissue, potentially leading to localised accumulation and controlled release of the drug from the silica carrier. This hypothesis could be confirmed through a real-time bioimaging study.

The methodology used in this study generates some concerns that must be highlighted, such as the amount of DSS consumed during the induction period, which naturally decreases over time because of the inflammatory condition [7,108], potentially introducing biases in the experiment. For example, the hurdles to individual control of water intake, as animals must remain in groups, can affect consistency. Nevertheless, DSS induction remains as one of the most efficient methods, with minimal or no animal mortality, making it a valuable option, especially when considering ethical aspects.

In summary, this study marks the first application of CUR and RSV loaded into MS particles in a UC induction model. The results from the

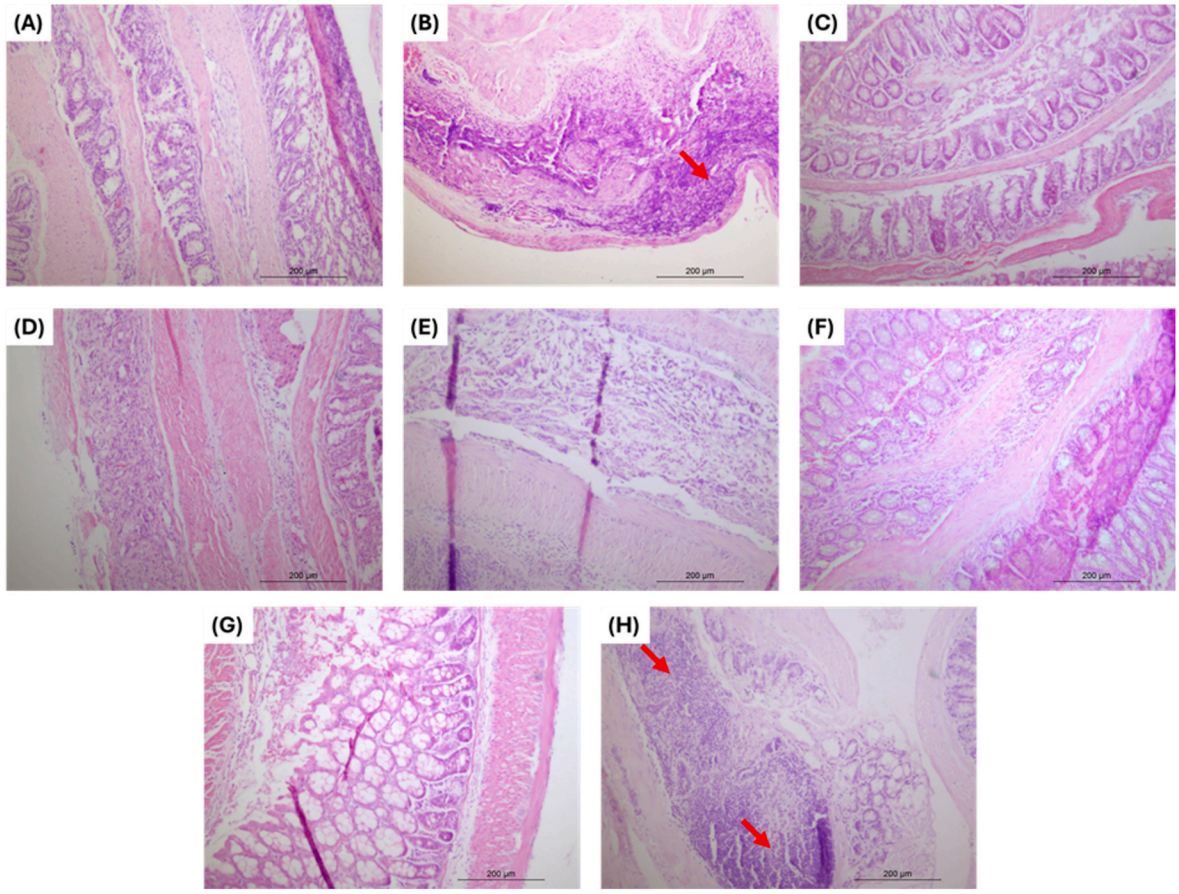

Fig. 12. Histological evaluation. **A**) Healthy (negative control); **B**) DSS (disease control); **C**) SULFA (100 mg/kg, positive control); **D**) MS-CUR (200 mg/kg); **E**) CUR (40 mg/kg); **F**) MS-RSV (200 mg/kg); **G**) RSV (40 mg/kg); **H**) MCM-41 (200 mg/kg, blank MS particles). Red arrows indicate severe leukocyte infiltration. Scale bar: 200 μm.

DSS colitis induction test demonstrated the enhanced activity of polyphenols when encapsulated into the pores of MS, with important improvements due to the impact of nanotechnology. Numerous studies have employed nanotechnological systems to deliver these polyphenols, particularly CUR, owing to its low permeability and solubility [21,87,109–114]. In cases where pharmacotechnical approaches are not used to modify the physicochemical properties of the drugs, other systems are employed aiming to improve the solubility of those compounds, even though some of them could be prejudicial for the organism, such as ethanol [74,76].

4. Conclusion

Natural active molecules such as polyphenols have interesting anti-inflammatory and antioxidant properties. However, their use is often limited due to solubility problems in aqueous and physiological media, which limits their potential translation to clinical practice for tackling inflammation-based conditions. The present work successfully addressed this problem in RSV and CUR as case studies by loading them into MS particles, which allow their partial amorphization as a consequence of the confinement effect. *In vitro* solubility and release studies confirmed that the semi-amorphised form of these drugs increased their solubility and extended the release time in comparison to the pure crystalline form. This controlled drug release behaviour is especially interesting for the purpose of achieving long-lasting therapies that enhance the local bioavailability of active ingredients in targeted tissues, thus reducing adverse side effects. As a representative inflammatory intestinal condition that urgently needs new therapeutic tools, due to its worldwide incidence and difficult management, a UC *in vivo* model was used to challenge the efficacy of polyphenol-loaded MS particles. The obtained DAI results revealed a marked symptom remission and partial reversion of the inflammatory process developed after UC induction, particularly for MS-CUR compared to non-encapsulated CUR. Furthermore, the reduction of locally expressed pro-inflammatory cytokines and cellular migration to the damaged tissues corroborated previous findings and confirmed the mitigation of intestinal inflammation.

This line of research introduces a promising new avenue for the treatment of UC, paving the way for future bioavailability studies and deepening our understanding of mesoporous silica-based drug delivery systems. These findings contribute to narrowing the gap towards the development of novel therapeutic strategies for UC. Overall, the findings reported herein demonstrate the pharmacological potential of polyphenol-loaded MS particles as a novel approach in the treatment of inflammatory conditions, especially bowel diseases. They offer a reliable alternative and complementary tool to conventional therapies such as corticosteroids, which present intrinsic side effects when used in long-term chronic cases.

CRediT authorship contribution statement

Renan Stein: Writing – original draft, Visualization, Validation, Methodology, Investigation, Formal analysis, Data curation, Conceptualization. **Miquel Martínez-Navarrete:** Writing – review & editing, Investigation. **Ana Paula Leão:** Writing – review & editing, Methodology, Conceptualization. **Ana Melero:** Writing – review & editing, Resources, Project administration, Methodology, Funding acquisition. **Silvio Buchner:** Writing – review & editing, Methodology, Formal analysis, Conceptualization. **Edilson Valmir Benvenutti:** Writing – review & editing, Methodology, Conceptualization. **Monique Deon:** Writing – review & editing, Project administration, Methodology, Conceptualization. **Antonio José Guillot:** Writing – review & editing, Methodology, Investigation, Conceptualization. **Ruy Carlos Ruver Beck:** Writing – review & editing, Visualization, Validation, Supervision, Resources, Project administration, Funding acquisition, Formal analysis, Data curation, Conceptualization.

Declaration of the use of generative AI and AI-assisted technologies in the writing process

The authors utilized ChatGPT to enhance language clarity and improve phrasing during the preparation of this manuscript. All content was subsequently reviewed and revised by the authors, who assume full responsibility for the final version of the work.

Declaration of competing interest

The authors declare that they have no known competing financial interests or personal relationships that could have appeared to influence the work reported in this paper.

Acknowledgements

This study is part of the National Institute of Science and Technology in 3D printing and Advanced Materials Applied to Human and Veterinary Health - INCT_3D-Saúde, funded by CNPq/Brazil (Grant #406436/2022-3). R. Stein thanks CAPES (Finance Code 001) and the National Council for Scientific and Technological Development – CNPq/Brazil (200172/2023-9) for PhD fellowships. This research was partially funded by DrugBiOp group of University of Valencia, Valencia, Spain. Figures were created using BioRender under active license.

Appendix A. Supplementary data

Supplementary data to this article can be found online at https://doi.org/10.1016/j.jddst.2025.107262.

Data availability

Data will be made available on request.

References

[1] C. Le Berre, S. Honap, L. Peyrin-Biroulet, Ulcerative colitis, Lancet 402 (10401) (2023 Aug 12) 571–584, https://doi.org/10.1016/S0140-6736(23)00966-2.
[2] R. Ungaro, S. Mehandru, P.B. Allen, L. Peyrin-Biroulet, J.F. Colombel, Ulcerative colitis, Lancet 389 (10080) (2017 Apr 29) 1756–1770, https://doi.org/10.1016/S0140-6736(16)32126-2.
[3] Kushal Seni, A. Saini, R. Debnath, A. Singh, A. Sharma, Singh Bisht Deepak, et al., Advancements in ulcerative colitis management: a critical assessment of etrasimod therapy, Health Sciences Review 12 (2024 Sep 1), https://doi.org/10.1016/j.hsr.2024.100196, 100196–6.
[4] T. Kucharzik, S. Koletzko, K. Kannengießer, A. Dignaß, Ulcerative colitis—diagnostic and therapeutic algorithms, Deutsches Aerzteblatt Online 117 (33–34) (2020 Aug 17) 564–574, https://doi.org/10.3238/arztebl.2020.0564.
[5] R.J. Porter, R. Kalla, G.T. Ho, Ulcerative colitis: recent advances in the understanding of disease pathogenesis, F1000Res 9 (2020 Apr 24), https://doi.org/10.12688/f1000research.20805.1. F1000 Faculty Rev-294.
[6] L. Du, C. Ha, Epidemiology and pathogenesis of ulcerative colitis, Gastroenterol. Clin. N. Am. 49 (4) (2020 Dec) 643–654, https://doi.org/10.1016/j.gtc.2020.07.005.
[7] F.R. Jaafar, A. Abu-Raghif, Comparative treatment of Sulfasalazine+Ezetimibe combination and Sulfasalazine in a rat model with induced colitis, J Med Life 16 (8) (2023 Aug) 1165–1169, https://doi.org/10.25122/jml-2023-0194.
[8] E. Coates, Nyantara Wickramasekera, A. Barr, P. Shackley, M. Lee, D. Hind, et al., Patient preferences and current practice for adults with steroid-resistant ulcerative colitis: POPSTER mixed-methods study, Health Technol. Assess. 26 (41) (2022) 1–118, https://doi.org/10.3310/RHXR5192, 1.
[9] Y. González, R. Mojica-Flores, D. Moreno-Labrador, L. Cubilla-Rios, K.S.J. Rao, P. L. Fernández, O.V. Larionov, J. Lakey-Beitia, Polyphenols with anti-inflammatory properties: synthesis and biological activity of novel curcumin derivatives, Int. J. Mol. Sci. 24 (4) (2023 Feb 12) 3691, https://doi.org/10.3390/ijms24043691.
[10] T.V. de Oliveira, R. Stein, D.F. de Andrade, R.C.R. Beck, Preclinical studies of the antitumor effect of curcumin-loaded polymeric nanocapsules: a systematic review and meta-analysis, Phytother Res. 36 (8) (2022 Aug) 3202–3214, https://doi.org/10.1002/ptr.7538.
[11] T. Meng, D. Xiao, A. Muhammed, J. Deng, L. Chen, J. He, Anti-inflammatory action and mechanisms of resveratrol, Molecules 26 (1) (2021) 229, https://doi.org/10.3390/molecules26010229, 5.
[12] I. Liguori, G. Russo, F. Curcio, G. Bulli, L. Aran, D. Della-Morte, G. Gargiulo, G. Testa, F. Cacciatore, D. Bonaduce, P. Abete, Oxidative stress, aging, and

diseases, Clin. Interv. Aging 13 (2018 Apr 26) 757–772, https://doi.org/10.2147/CIA.S158513.
[13] S. Galiniak, et al., Clinical aspects of protein glycation, European Journal of Clinical and Experimental Medicine 15 (3) (2018) 263–267, https://doi.org/10.15584/ejcem.2017.3.10.
[14] L. Zeng, T. Yang, K. Yang, G. Yu, J. Li, W. Xiang, et al., Curcumin and curcuma longa extract in the treatment of 10 types of autoimmune diseases: a systematic review and meta-analysis of 31 randomized controlled trials, Frontiers in Immunology [Internet] 13 (2022 Aug 1) 896476, https://doi.org/10.3389/fimmu.2022.896476.
[15] J. Yang, X. Chen, J. Lin, et al., Co-delivery of resveratrol and curcumin based on Mesona chinensis polysaccharides/zein nanoparticle for targeted alleviation of ulcerative colitis, Food Biosci. 59 (2024), https://doi.org/10.1016/j.fbio.2024.104060.
[16] B.X. Yang, L. Li, G. Shang, M. Zhuo, H. Zhu, S. Xu, J. Zhao, X. Hou, Y. Shi, Oral curcumin through mesoporous silica nanomaterials with distinct morphologies: synthesis, characterization, biosafety evaluation, and antioxidant activity in vivo, Langmuir 40 (52) (2024) 27216–27227, https://doi.org/10.1021/acs.langmuir.4c02871. Dec 31.
[17] R. de A. Goulart, S.M. Barbalho, C.J. Rubira, A.C. Araújo, V.M. Lima, R. L. Buchaim, et al., Curcumin therapy for ulcerative colitis remission: systematic review and meta-analysis, Expet Rev. Gastroenterol. Hepatol. 14 (12) (2020 Aug 24) 1171–1179, https://doi.org/10.1080/17474124.2020.1808460.
[18] V. Gowd, Jori C. Kanika, A.A. Chaudhary, H.A. Rudayni, S. Rashid, R. Khan, Resveratrol and resveratrol nano-delivery systems in the treatment of inflammatory bowel disease, J. Nutr. Biochem. 109 (2022 Nov) 109101, https://doi.org/10.1016/j.jnutbio.2022.109101.
[19] S.V. Luca, I. Macovei, A. Bujor, A. Miron, K. Skalicka-Woźniak, A.C. Aprotosoaie, et al., Bioactivity of dietary polyphenols: the role of metabolites, Crit. Rev. Food Sci. Nutr. 60 (4) (2019) 626–659, https://doi.org/10.1080/10408398.2018.1546669, 7.
[20] K.U. Pandey, S.V. Dalvi, Understanding stability relationships among three curcumin polymorphs, Adv. Powder Technol. 30 (2) (2019) 266–276, https://doi.org/10.1016/j.apt.2018.11.002.
[21] C. Wang, Z. Han, Y. Wu, X. Lu, X. Tang, J. Xiao, et al., Enhancing stability and anti-inflammatory properties of curcumin in ulcerative colitis therapy using liposomes mediated colon-specific drug delivery system, Food Chem. Toxicol. 151 (2021 May) 112123, https://doi.org/10.1016/j.fct.2021.112123.
[22] E. Rastegari, Y.J. Hsiao, W.Y. Lai, Y.H. Lai, T.C. Yang, S.J. Chen, P.I. Huang, S. H. Chiou, C.Y. Mou, Y. Chien, An update on mesoporous silica nanoparticle applications in nanomedicine, Pharmaceutics 13 (7) (2021 Jul 12) 1067, https://doi.org/10.3390/pharmaceutics13071067.
[23] M. Vallet-Regí, M. Colilla, I. Izquierdo-Barba, M. Manzano, Mesoporous silica nanoparticles for drug delivery: current insights, Molecules 23 (1) (2017 Dec 25) 47, https://doi.org/10.3390/molecules23010047.
[24] Y.D. Deng, X.D. Zhang, X.S. Yang, Z.L. Huang, X. Wei, X.F. Yang, W.Z. Liao, Subacute toxicity of mesoporous silica nanoparticles to the intestinal tract and the underlying mechanism, J. Hazard Mater. 409 (2021 May 5) 124502, https://doi.org/10.1016/j.jhazmat.2020.124502.
[25] M. Heidari Nia, R. Koshani, J.G. Munguia-Lopez, A.R. Kiasat, J.M. Kinsella, T.G. M. van de Ven, Biotemplated hollow mesoporous silica particles as efficient carriers for drug delivery, ACS Appl. Bio Mater. 4 (5) (2021 May 17) 4201–4214, https://doi.org/10.1021/acsabm.0c01671.
[26] Marzieh Heidari Nia, Roya Koshani, J.G. Munguia-Lopez, Reza Kiasat Ali, J. M. Kinsella, Theo. Biotemplated hollow mesoporous silica particles as efficient carriers for drug delivery, ACS Appl. Bio Mater. 4 (5) (2021 Apr 27) 4201–4214, https://doi.org/10.1021/acsabm.0c01671.
[27] E. Hagman, A. Elimam, N. Kupferschmidt, K. Ekbom, S. Rössner, M.N. Iqbal, E. Johnston, M. Lindgren, T. Bengtsson, P. Danielsson, Oral intake of mesoporous silica is safe and well tolerated in male humans, PLoS One 15 (10) (2020 Oct 2) e0240030, https://doi.org/10.1371/journal.pone.0240030.
[28] B. Xu, S. Li, R. Shi, H. Liu, Multifunctional mesoporous silica nanoparticles for biomedical applications, Signal Transduct. Targeted Ther. 8 (1) (2023 Nov 24), https://doi.org/10.1038/s41392-023-01654-7.
[29] S. Mendiratta, M. Hussein, H.A. Nasser, A.A.A. Ali, Multidisciplinary role of mesoporous silica nanoparticles in brain regeneration characterization and cancers: from crossing the blood-brain barrier to treatment. Particle & particle systems, [S.L.] 36 (9) (2019) 298–319, https://doi.org/10.1002/ppsc.201900195.
[30] M. Iranshahy, et al., Curcumin-loaded mesoporous silica nanoparticles for drug delivery: synthesis, biological assays and therapeutic potential – a review, RSC Adv. 13 (2023) 22250, https://doi.org/10.1039/d3ra02772d.
[31] M.K.M. Esfahani, S.E. Alavi, P.J. Cabot, N. Islam, E.L. Izake, PEGylated mesoporous silica nanoparticles (MCM-41): a promising carrier for the targeted delivery of fenbendazole into prostrate cancer cells, Pharmaceutics 13 (10) (2021 Oct 2) 1605, https://doi.org/10.3390/pharmaceutics13101605.
[32] S. Kim, R. Diab, O. Joubert, N. Canilho, A. Pasc, Core-shell microcapsules of solid lipid nanoparticles and mesoporous silica for enhanced oral delivery of curcumin, Colloids Surf. B Biointerfaces 140 (2016 Apr 1) 161–168, https://doi.org/10.1016/j.colsurfb.2015.12.040.
[33] Y. Gao, S. Ding, X. Huang, Z. Fan, J. Sun, Y. Hai, K. Li, Development and evaluation of hollow mesoporous silica microspheres bearing on enhanced oral delivery of curcumin, Drug Dev. Ind. Pharm. 45 (2) (2019 Feb) 273–281, https://doi.org/10.1080/03639045.2018.1539098.
[34] M. Grün, U. K.K, A. Matsumoto, K. Tsutsumi, Novel pathways for the preparation of mesoporous MCM-41 materials: control of porosity and morphology, Microporous Mesoporous Mater. 27 (2–3) (1999) 207–216, https://doi.org/10.1016/S1387-1811(98)00255-8.
[35] Z. Li, Y. Zhang, N. Feng, Mesoporous silica nanoparticles: synthesis, classification, drug loading, pharmacokinetics, biocompatibility, and application in drug delivery, Expet Opin. Drug Deliv. 16 (3) (2019 Mar) 219–237, https://doi.org/10.1080/17425247.2019.1575806.
[36] K. Coradini, F.O. Lima, C.M. Oliveira, P.S. Chaves, M.L. Athayde, L.M. Carvalho, R.C. Beck, Co-encapsulation of resveratrol and curcumin in lipid-core nanocapsules improves their in vitro antioxidant effects, Eur. J. Pharm. Biopharm. 88 (1) (2014 Sep) 178–185, https://doi.org/10.1016/j.ejpb.2014.04.009.
[37] K. Mladenovska, R.S. Raicki, E.I. Janevik, T. Ristoski, M.J. Pavlova, Z. Kavrakovski, M.G. Dodov, K. Goracinova, Colon-specific delivery of 5-amino-salicylic acid from chitosan-Ca-alginate microparticles, Int. J. Pharm. 342 (1–2) (2007 Sep 5) 124–136, https://doi.org/10.1016/j.ijpharm.2007.05.028.
[38] J. Arasa, P. Martos, M.C. Terencio, F. Valcuende-Cavero, M.C. Montesinos, Topical application of the adenosine A2A receptor agonist CGS-21680 prevents phorbol-induced epidermal hyperplasia and inflammation in mice, Exp. Dermatol. 23 (8) (2014 Aug) 555–560, https://doi.org/10.1111/exd.12461.
[39] Matthias Thommes, Katsumi Kaneko, Alexander V. Neimark, James P. Olivier, Francisco Rodriguez-Reinoso, Jean Rouquerol, Kenneth S.W. Sing, Physisorption of gases, with special reference to the evaluation of surface area and pore size distribution (IUPAC Technical Report), Pure Appl. Chem. 87 (9–10) (2015) 1051–1069, https://doi.org/10.1515/pac-2014-1117.
[40] R.M. Sábio, S.H. Santagneli, M. Gressier, J.M.A. Caiut, W.M. Pazin, I.S. Leite, N. M. Inada, R. Rosa da Silva, S.J.L. Ribeiro, M.J. Menu, Luminescent nanohybrids based on silica and silylated Ru (II)-Yb(III) heterobinuclear complex: new tools for biological media analysis, Nanotechnology 31 (8) (2019 Nov 8) 085709, https://doi.org/10.1088/1361-6528/ab55c3.
[41] T.C. Ribeiro, R.M. Sábio, M.T. Luiz, L.C. de Souza, B. Fonseca-Santos, L.C. Cides da Silva, M.C.A. Fantini, C.D.S. Planeta, M. Chorilli, Curcumin-loaded mesoporous silica nanoparticles dispersed in thermo-responsive hydrogel as potential alzheimer disease therapy, Pharmaceutics 14 (9) (2022 Sep 19) 1976, https://doi.org/10.3390/pharmaceutics14091976.
[42] X. Jiang, X. Liu, Q. Yu, W. Shen, X. Mei, H. Tian, C. Wu, Functional resveratrol-biodegradable manganese doped silica nanoparticles for the spinal cord injury treatment, Mater. Today Bio 13 (2021 Dec 4) 100177, https://doi.org/10.1016/j.mtbio.2021.100177.
[43] S.B. Hartono, et al., Porous silica nanoparticles as carrier for curcumin delivery, AIP Conf. Proc. (2018) 1–7, https://doi.org/10.1063/1.5030229.
[44] J.S. Beck, et al., A new family of mesoporous molecular sieves prepared with liquid crystal templates, J. Am. Chem. Soc. 114 (27) (1992) 10834–10843, https://doi.org/10.1021/ja00053a020.
[45] M.C. Velho, N.L. Funk, M. Deon, E.V. Benvenutti, S. Buchner, R. Hinrichs, D. A. Pilger, R.C.R. Beck, Ivermectin-loaded mesoporous silica and polymeric nanocapsules: impact on drug loading, in vitro solubility enhancement, and release performance, Pharmaceutics 16 (3) (2024 Feb 26) 325, https://doi.org/10.3390/pharmaceutics16030325.
[46] V. Dubovoy, R. Subramanyam, M. Stranick, L. Du-Thumm, L. Pan, Facile preparation of ultrafine aluminum hydroxide particles with or without mesoporous MCM-41 in ambient environments, J. Vis. Exp. 11 (123) (2017 May) 55423, https://doi.org/10.3791/55423.
[47] G.J. Soler-Illia, O. Azzaroni, Multifunctional hybrids by combining ordered mesoporous materials and macromolecular building blocks, Chem. Soc. Rev. 40 (2) (2011 Feb) 1107–1150, https://doi.org/10.1039/c0cs00208a.
[48] N.L. Funk, et al., Naproxen-loaded mesoporous silica nanoparticles: how can the process of incorporation affect drug placement, drug release and the in vitro naproxen irritant potential? Microporous Mesoporous Mater. 384 (2025) 113458 https://doi.org/10.1016/j.micromeso.2024.113458.
[49] N. Summerlin, Z. Qu, N. Pujara, Y. Sheng, S. Jambhrunkar, M. McGuckin, A. Popat, Colloidal mesoporous silica nanoparticles enhance the biological activity of resveratrol, Colloids Surf. B Biointerfaces 144 (2016 Aug 1) 1–7, https://doi.org/10.1016/j.colsurfb.2016.03.076.
[50] A.H. Ibrahim, J.H. Smått, N.P. Govardhanam, H.M. Ibrahim, H.R. Ismael, M. I. Afouna, et al., Formulation and optimization of drug-loaded mesoporous silica nanoparticle-based tablets to improve the dissolution rate of the poorly water-soluble drug silymarin, Eur. J. Pharmaceut. Sci. 142 (2020 Jan) 105103, https://doi.org/10.1016/j.ejps.2019.105103.
[51] C.A. McCarthy, R.J. Ahern, R. Dontireddy, K.B. Ryan, A.M. Crean, Mesoporous silica formulation strategies for drug dissolution enhancement: a review, Expet Opin. Drug Deliv. 13 (1) (2016) 93–108, https://doi.org/10.1517/17425247.2016.1100165.
[52] N.P. Aditya, Ian E. Hamilton, Ian T. Norton, Amorphous nano-curcumin stabilized oil in water emulsion: physico chemical characterization, Food Chem. 224 (2017) 191–200, https://doi.org/10.1016/j.foodchem.2016.12.082.
[53] S. Basile, E. Mathew, I. Genta, B. Conti, R. Dorati, D.A. Lamprou, Optimization of FDM 3D printing process parameters to produce haemodialysis curcumin-loaded vascular grafts, Drug Deliv Transl Res 13 (8) (2023 Aug) 2058–2071, https://doi.org/10.1007/s13346-021-01078-2.
[54] C. Kececiler-Emir, E. Ilhan-Ayisigi, C. Celen-Erden, A. Nalbantsoy, O. Yesil-Celiktas, Synthesis of resveratrol loaded hybrid silica-PAMAM dendrimer nanoparticles with emphases on inducible nitric oxide synthase and cytotoxicity, Plant Foods Hum. Nutr. 76 (2) (2021 Jun) 219–225, https://doi.org/10.1007/s11130-021-00897-5.
[55] I. Trendafilova, R. Chimshirova, D. Momekova, H. Petkov, N. Koseva, P. Petrova, M. Popova, Curcumin and capsaicin-loaded Ag-modified mesoporous silica

carriers: a new alternative in skin treatment, Nanomaterials 12 (17) (2022 Sep 5) 3075, https://doi.org/10.3390/nano12173075.
[56] C. Scheid, W. Mello, S. Buchner, E.V. Benvenutti, M. Deon, Josias Merib, Efficient analysis of polycyclic aromatic hydrocarbons by dispersive-μ-solid-phase extraction using silica-based nanostructured sorbent phases coupled to gas chromatography-mass spectrometry, Advances in Sample Preparation 7 (2023 May 10), https://doi.org/10.1016/j.sampre.2023.100070, 100070–0.
[57] M. Lin, W. Yao, Y. Xiao, Z. Dong, W. Huang, F. Zhang, X. Zhou, M. Liang, Resveratrol-modified mesoporous silica nanoparticle for tumor-targeted therapy of gastric cancer, Bioengineered 12 (1) (2021 Dec) 6343–6353, https://doi.org/10.1080/21655979.2021.1971507.
[58] L. Harini, B. Karthikeyan, S. Srivastava, S.B. Suresh, C. Ross, G. Gnanakumar, S. Rajagopal, K. Sundar, T. Kathiresan, Polyethylenimine-modified curcumin-loaded mesoporus silica nanoparticle (MCM-41) induces cell death in MCF-7 cell line, IET Nanobiotechnol. 11 (1) (2017 Feb) 57–61, https://doi.org/10.1049/iet-nbt.2016.0075.
[59] L. Qin, Y. He, X. Zhao, T. Zhang, Y. Qin, A. Du, Preparation, characterization, and in vitro sustained release profile of resveratrol-loaded silica aerogel, Molecules 25 (12) (2020 Jun 15) 2752, https://doi.org/10.3390/molecules25122752.
[60] C. Chen, W. Sun, X. Wang, Y. Wang, P. Wang, Rational design of curcumin loaded multifunctional mesoporous silica nanoparticles to enhance the cytotoxicity for targeted and controlled drug release, Mater. Sci. Eng., C 85 (2018 Apr 1) 88–96, https://doi.org/10.1016/j.msec.2017.12.007.
[61] Y. Hu, Z. Wang, Y. Qiu, Y. Liu, M. Ding, Y. Zhang, Anti-miRNA21 and resveratrol-loaded polysaccharide-based mesoporous silica nanoparticle for synergistic activity in gastric carcinoma, J. Drug Target. 27 (10) (2019 Dec) 1135–1143, https://doi.org/10.1080/1061186X.2019.1610766.
[62] S. Jambhrunkar, Z. Qu, A. Popat, J. Yang, O. Noonan, L. Acauan, Y. Ahmad Nor, C. Yu, S. Karmakar, Effect of surface functionality of silica nanoparticles on cellular uptake and cytotoxicity, Mol. Pharm. 11 (10) (2014 Oct 6) 3642–3655, https://doi.org/10.1021/mp500385n.
[63] M.A. Rahman, A. Ali, M. Rahamathulla, S. Salam, U. Hani, S. Wahab, M.H. Warsi, M. Yusuf, A. Ali, V. Mittal, R.K. Harwansh, Fabrication of sustained release curcumin-loaded solid lipid nanoparticles (Cur-SLNs) as a potential drug delivery system for the treatment of lung cancer: optimization of formulation and in vitro biological evaluation, Polymers (Basel) 15 (3) (2023 Jan 20) 542, https://doi.org/10.3390/polym15030542.
[64] Wenjing Zhu, Wenling Fan, Xiaotong Zhang, Meiqi Gao, Sustained-release solid dispersion of high-melting-point and insoluble resveratrol prepared through hot melt extrusion to improve its solubility and bioavailability, Molecules 26 (2021) 4982, https://doi.org/10.3390/molecules26164982.
[65] T. Heikkilä, J. Salonen, J. Tuura, N. Kumar, T. Salmi, D.Y. Murzin, M.S. Hamdy, G. Mul, L. Laitinen, A.M. Kaukonen, J. Hirvonen, V.P. Lehto, Evaluation of mesoporous TCPSi, MCM-41, SBA-15, and TUD-1 materials as API carriers for oral drug delivery, Drug Deliv. 14 (6) (2007 Aug) 337–347, https://doi.org/10.1080/10717540601098823.
[66] T. Limnell, T. Heikkilä, H.A. Santos, S. Sistonen, S. Hellstén, T. Laaksonen, L. Peltonen, N. Kumar, D.Y. Murzin, M. Louhi-Kultanen, J. Salonen, J. Hirvonen, V.P. Lehto, Physicochemical stability of high indomethacin payload ordered mesoporous silica MCM-41 and SBA-15 microparticles, Int. J. Pharm. 416 (1) (2011 Sep 15) 242–251, https://doi.org/10.1016/j.ijpharm.2011.06.050.
[67] R. Mellaerts, C.A. Aerts, J. Van Humbeeck, P. Augustijns, G. Van den Mooter, J. A. Martens, Enhanced release of itraconazole from ordered mesoporous SBA-15 silica materials, Chem Commun (Camb) (13) (2007 Apr 7) 1375–1377, https://doi.org/10.1039/b616746b.
[68] S.S. Hate, S.M. Reutzel-Edens, L.S. Taylor, Influence of drug-silica electrostatic interactions on drug release from mesoporous silica-based oral delivery systems, Mol. Pharm. 17 (9) (2020 Sep 8) 3435–3446, https://doi.org/10.1021/acs.molpharmaceut.0c00488.
[69] R. Rai, C. Merrell, W. Yokoyama, N. Nitin, Infusion of trans-resveratrol in micron-scale grape skin powder for enhanced stability and bioaccessibility, Food Chem. 340 (2021 Mar 15) 127894, https://doi.org/10.1016/j.foodchem.2020.127894.
[70] S. Manju, K. Sreenivasan, Conjugation of curcumin onto hyaluronic acid enhances its aqueous solubility and stability, J. Colloid Interface Sci. 359 (1) (2011 Jul 1) 318–325, https://doi.org/10.1016/j.jcis.2011.03.071.
[71] K. Coradini, R.B. Friedrich, F.N. Fonseca, M.S. Vencato, D.F. Andrade, C. M. Oliveira, A.P. Battistel, S.S. Guterres, M.I. da Rocha, A.R. Pohlmann, R. C. Beck, A novel approach to arthritis treatment based on resveratrol and curcumin co-encapsulated in lipid-core nanocapsules: in vivo studies, Eur. J. Pharmaceut. Sci. 78 (2015 Oct 12) 163–170, https://doi.org/10.1016/j.ejps.2015.07.012.
[72] N. Pujara, R. Giri, K.Y. Wong, Z. Qu, P. Rewatkar, M. Moniruzzaman, J. Begun, B. P. Ross, M. McGuckin, A. Popat, pH - responsive colloidal carriers assembled from β-lactoglobulin and Epsilon poly-L-lysine for oral drug delivery, J. Colloid Interface Sci. 589 (2021 May) 45–55, https://doi.org/10.1016/j.jcis.2020.12.054.
[73] M.R. Shin, K.J. Kim, S.H. Kim, S.J. Kim, B.I. Seo, H.J. An, S.S. Roh, Comparative evaluation between sulfasalazine alone and in combination with herbal medicine on DSS-induced ulcerative colitis mice, BioMed Res. Int. 2017 (2017) 6742652, https://doi.org/10.1155/2017/6742652.
[74] J. Yao, J. Wang, L. Liu, Y.X. Li, Xun An-Ying, W.S. Zeng, et al., Anti-oxidant effects of resveratrol on mice with DSS-induced ulcerative colitis, Arch. Med. Res. 41 (4) (2010 May 1) 288–294, https://doi.org/10.1016/j.arcmed.2010.05.002.
[75] M. Samsamikor, N.E. Daryani, P.R. Asl, A. Hekmatdoost, Resveratrol supplementation and oxidative/anti-oxidative status in patients with ulcerative colitis: a randomized, double-blind, placebo-controlled pilot study, Arch. Med. Res. (2016 May 1), https://doi.org/10.1016/j.arcmed.2016.07.003.
[76] M. Samsamikor, Naser Ebrahimi Daryani, Parisa Rezanejad Asl, Azita Hekmatdoost, Anti-inflammatory effects of resveratrol in patients with ulcerative colitis: a randomized, double-blind, placebo-controlled pilot, Study 46 (4) (2015 May 1) 280–285, https://doi.org/10.1016/j.arcmed.2015.05.005.
[77] R.A. Goulart, S.M. Barbalho, V.M. Lima, G.A. Souza, J.N. Matias, A.C. Araújo, C. J. Rubira, R.L. Buchaim, D.V. Buchaim, A.C.A. Carvalho, É.L. Guiguer, Effects of the use of curcumin on ulcerative colitis and crohn's disease: a systematic review, J. Med. Food 24 (7) (2021 Jul) 675–685, https://doi.org/10.1089/jmf.2020.0129.
[78] J. Yin, L. Wei, N. Wang, X. Li, M. Miao, Efficacy and safety of adjuvant curcumin therapy in ulcerative colitis: a systematic review and meta-analysis, J. Ethnopharmacol. 289 (2022 May 10) 115041, https://doi.org/10.1016/j.jep.2022.115041.
[79] C. Wei, J.Y. Wang, F. Xiong, B.H. Wu, M.H. Luo, Z.C. Yu, et al., Curcumin ameliorates DSS-induced colitis in mice by regulating the Treg/Th17 signaling pathway, Mol. Med. Rep. 23 (1) (2020 Nov 9), https://doi.org/10.3892/mmr.2020.11672, 1–1.
[80] C.P. Li, J.H. Li, S.Y. He, O. Chen, L. Shi, Effect of curcumin on p38MAPK expression in DSS-induced murine ulcerative colitis, Genet. Mol. Res. 14 (2) (2015) 3450–3458, https://doi.org/10.4238/2015.April.15.8.
[81] H. Hanai, T. Iida, K. Takeuchi, F. Watanabe, Y. Maruyama, A. Andoh, et al., Curcumin maintenance therapy for ulcerative colitis: randomized, multicenter, double-blind, placebo-controlled trial, Clin. Gastroenterol. Hepatol. 4 (12) (2006 Dec) 1502–1506, https://doi.org/10.1016/j.cgh.2006.08.008.
[82] R. Banerjee, P. Pal, A. Penmetsa, P. Kathi, G. Girish, I. Goren, et al., Novel bioenhanced curcumin with mesalamine for induction of clinical and endoscopic remission in mild-to-moderate ulcerative colitis, J. Clin. Gastroenterol. (2020 Sep 4), https://doi.org/10.1097/MCG.0000000000001416. Publish Ahead of Print.
[83] S. Kedia, V. Bhatia, S. Thareja, S. Garg, V.P. Mouli, S. Bopanna, et al., Low dose oral curcumin is not effective in induction of remission in mild to moderate ulcerative colitis: results from a randomized double-blind placebo-controlled trial, World J. Gastrointest. Pharmacol. Therapeut 8 (2) (2017) 147, https://doi.org/10.4292/wjgpt.v8i2.147.
[84] B. Yu, Y. Wang, Z. Tan, Z. Hong, L. Yao, S. Huang, et al., Resveratrol ameliorates DSS-induced ulcerative colitis by acting on mouse gut microbiota, Inflammopharmacology 32 (3) (2024 Mar 16) 2023–2033, https://doi.org/10.1007/s10787-024-01456-5.
[85] X. Yu, X. Li, Y. Xu, Y. Li, Y. Zhou, J. Zhang, et al., Resveratrol ameliorates ulcerative colitis by upregulating Nrf2/HO-1 pathway activity: integrating animal experiments and network pharmacology, Mol. Med. Rep. 29 (5) (2024 Mar 14), https://doi.org/10.3892/mmr.2024.13201.
[86] C. Gao, Y. Zhou, Z. Chen, H. Li, Y. Xiao, W. Hao, et al., Turmeric-derived nanovesicles as novel nanobiologics for targeted therapy of ulcerative colitis, Theranostics [Internet] 12 (12) (2022) 5596–5614, https://doi.org/10.7150/thno.73650.
[87] B. Xiao, X. Si, M. Zhang, D. Merlin, Oral Administration of pH-Sensitive Curcumin-Loaded Microparticles for Ulcerative Colitis Therapy, 2015 Nov 1, https://doi.org/10.1016/j.colsurfb.2015.07.081.
[88] A. Ohtsu, Y. Shibutani, K. Seno, H. Iwata, T. Kuwayama, K. Shirasuna, Advanced glycation end products and lipopolysaccharides stimulate interleukin-6 secretion via the RAGE/TLR4-NF-κB-ROS pathways and resveratrol attenuates these inflammatory responses in mouse macrophages, Exp. Ther. Med. 14 (5) (2017 Nov) 4363–4370, https://doi.org/10.3892/etm.2017.5045.
[89] S. Akyuz, F. Turan, L. Gurbuzler, A. Arici, E. Sogut, O. Ozkan, The anti-inflammatory and antioxidant effects of curcumin in Middle ear infection, J. Craniofac. Surg. 27 (5) (2016 Jul) e494–e497, https://doi.org/10.1097/SCS.0000000000002810.
[90] A. Gupta, L.D. Kagliwal, R.S. Singhal, Biotransformation of polyphenols for improved bioavailability and processing stability, Adv. Food Nutr. Res. (2013) 183–217, https://doi.org/10.1016/B978-0-12-410540-9.00004-1.
[91] Z. Chaudhary, et al., Encapsulation and controlled release of resveratrol within functionalized mesoporous silica nanoparticles for prostate cancer therapy, Front. Bioeng. Biotechnol. 7 (2019) 1–9, https://doi.org/10.3389/fbioe.2019.00225.
[92] Özge Erol Doğan, Kezban Esen Karaca Çelik, Murat Baş, Eyüp Hakan Alan, Yasir Furkan Çağın, Effects of mediterranean diet, curcumin, and resveratrol on mild-to-moderate active ulcerative colitis: a multicenter randomized clinical trial, Nutrients 16 (10) (2024 May 16), https://doi.org/10.3390/nu16101504, 1504–4.
[93] M.L.Y. Wan, V.A. Co, H. El-Nezami, Dietary polyphenol impact on gut health and microbiota, Crit. Rev. Food Sci. Nutr. 61 (4) (2020 Mar 25) 690–711, https://doi.org/10.1080/10408398.2020.1744512.
[94] P. Dogra, N.L. Adolphi, Z. Wang, Y.S. Lin, K.S. Butler, P.N. Durfee, J.G. Croissant, A. Noureddine, E.N. Coker, E.L. Bearer, V. Cristini, C.J. Brinker, Establishing the effects of mesoporous silica nanoparticle properties on in vivo disposition using imaging-based pharmacokinetics, Nat. Commun. 9 (1) (2018 Oct 31) 4551, https://doi.org/10.1038/s41467-018-06730-z.
[95] S.Y.J. Tam, J.K. Coller, A. Wignall, R.J. Gibson, A. Khatri, C. Barbé, J.M. Bowen, Intestinal accumulation of silica particles in a rat model of dextran sulfate sodium-induced colitis, Ann. Gastroenterol. 32 (6) (2019 Nov-Dec) 584–592, https://doi.org/10.20524/aog.2019.0411.
[96] A.H. Teruel, É. Pérez-Esteve, I. González-Álvarez, M. González-Álvarez, A. M. Costero, D. Ferri, P. Gaviña, V. Merino, R. Martínez-Máñez, F. Sancenón, Double drug delivery using capped mesoporous silica microparticles for the

effective treatment of inflammatory bowel disease, Mol. Pharm. 16 (6) (2019 Jun 3) 2418–2429, https://doi.org/10.1021/acs.molpharmaceut.9b00041.
[97] S.V. Rana, S. Sharma, J. Kaur, K.K. Prasad, S.K. Sinha, R. Kochhar, et al., Relationship of cytokines, oxidative stress and GI motility with bacterial overgrowth in ulcerative colitis patients, Journal of Crohn's and Colitis 8 (8) (2014 Aug) 859–865, https://doi.org/10.1016/j.crohns.2014.01.007.
[98] J.C. Hoving, R. Keeton, M.A. Höft, M. Ozturk, P. Otieno-Odhiambo, F. Brombacher, IL-4 receptor-alpha signalling of intestinal epithelial cells, smooth muscle cells, and macrophages plays a redundant role in oxazolone colitis, Mediat. Inflamm. 2020 (2020 Jan 17) 1–11, https://doi.org/10.1155/2020/4361043.
[99] Yao Hui-yuan, F. Wang, H. Chong, J. Wang, Y. Bai, M. Du, et al., A curcumin-modified coordination polymers with ROS scavenging and macrophage phenotype regulating properties for efficient ulcerative colitis treatment, Adv. Sci. 10 (19) (2023 May 17), https://doi.org/10.1002/advs.202300601.
[100] Milad Sabzevary-Ghahfarokhi, A. Soltani, F. Luzza, T. Larussa, G. Rahimian, Hedayatollah Shirzad, et al., The protective effects of resveratrol on ulcerative colitis via changing the profile of Nrf2 and IL-1β protein, Mol. Biol. Rep. 47 (9) (2020 Sep 1) 6941–6947, https://doi.org/10.1007/s11033-020-05753-4.
[101] A. Mizoguchi, E. Mizoguchi, A.K. Bhan, The critical role of interleukin 4 but not interferon gamma in the pathogenesis of colitis in T-cell receptor α mutant mice, Gastroenterology 116 (2) (1999 Feb) 320–326, https://doi.org/10.1016/s0016-5085(99)70128-9.
[102] L. Stevceva, P. Pavli, A. Husband, A. Ramsay, W. Doe, Dextran sulphate sodium-induced colitis is ameliorated in interleukin 4 deficient mice, Gene Immun. 2 (6) (2001 Oct 1) 309–316, https://doi.org/10.1038/sj.gene.6363782.
[103] F. Heller, P. Florian, C. Bojarski, J. Richter, M. Christ, B. Hillenbrand, et al., Interleukin-13 is the key effector Th2 cytokine in ulcerative colitis that affects epithelial tight junctions, apoptosis, and cell restitution, Gastroenterology 129 (2) (2005 Aug) 550–564, https://doi.org/10.1053/j.gastro.2005.05.002.
[104] E.P. Karmele, T.S. Pasricha, T.R. Ramalingam, R.W. Thompson, R.L. Gieseck 3rd, K.J. Knilans, M. Hegen, M. Farmer, F. Jin, A. Kleinman, D.A. Hinds, , 23andMe Research Team, T. Almeida Pereira, R. de Queiroz Prado, N. Bing, L. Tchistiakova, M.T. Kasaian, T.A. Wynn, K.M. Vannella, Anti-IL-13Rα2 therapy promotes recovery in a murine model of inflammatory bowel disease, Mucosal Immunol. 12 (5) (2019 Sep) 1174–1186, https://doi.org/10.1038/s41385-019-0189-6.
[105] M. Hoffmann, U. Schwertassek, A. Seydel, K. Weber, W. Falk, S. Hauschildt, J. Lehmann, A refined and translationally relevant model of chronic DSS colitis in BALB/c mice, Lab. Anim 52 (3) (2018 Jun) 240–252, https://doi.org/10.1177/0023677217742681.
[106] F. Yasmin, H. Najeeb, S. Shaikh, M. Hasanain, U. Naeem, A. Moeed, T. Koritala, S. Hasan, S. Surani, Novel drug delivery systems for inflammatory bowel disease, World J. Gastroenterol. 28 (18) (2022 May 14) 1922–1933, https://doi.org/10.3748/wjg.v28.i18.1922.
[107] H.F. Chiu, K. Venkatakrishnan, O. Golovinskaia, C.K. Wang, Gastroprotective effects of polyphenols against various gastro-intestinal disorders: a mini-review with special focus on clinical evidence, Molecules 26 (7) (2021 Apr 6) 2090, https://doi.org/10.3390/molecules26072090.
[108] L.A. Dieleman, B.U. Ridwan, G.S. Tennyson, K.W. Beagley, R.P. Bucy, C.O. Elson, Dextran sulfate sodium-induced colitis occurs in severe combined immunodeficient mice, Gastroenterology 107 (6) (1994 Dec) 1643–1652, https://doi.org/10.1016/0016-5085(94)90803-6.
[109] X. Liu, et al., Advances in antioxidant nanozymes for biomedical applications, Coord. Chem. Rev. 502 (2024) 215610, https://doi.org/10.1016/j.ccr.2023.215610.
[110] D. Hales, D.M. Muntean, M.A. Neag, B. Kiss, M.G. Ştefan, L.R. Tefas, et al., Curcumin-loaded microspheres are effective in preventing oxidative stress and intestinal inflammatory abnormalities in experimental ulcerative colitis in rats, Molecules 27 (17) (2022 Sep 2) 5680, https://doi.org/10.3390/molecules27175680.
[111] C. Quispe, N. Cruz-Martins, M.L. Manca, M. Manconi, O. Sytar, N. Hudz, M. Shanaida, M. Kumar, Y. Taheri, M. Martorell, J. Sharifi-Rad, G. Pintus, W. C. Cho, Nano-derived therapeutic formulations with curcumin in inflammation-related diseases, Oxid. Med. Cell. Longev. 2021 (2021 Sep 15) 3149223, https://doi.org/10.1155/2021/3149223.
[112] Q. Chenb, S. Gou, P. Ma, H. Song, X. Zhou, Y. Huang, et al., Oral administration of colitis tissue-accumulating porous nanoparticles for ulcerative colitis therapy, Int. J. Pharm. 557 (2019 Feb) 135–144, https://doi.org/10.1016/j.ijpharm.2018.12.046.
[113] A. Melero, C. Draheim, S. Hansen, E. Giner, J.J. Carreras, R. Talens-Visconti, T. M. Garrigues, J.E. Peris, M.C. Recio, R. Giner, C.M. Lehr, Targeted delivery of Cyclosporine A by polymeric nanocarriers improves the therapy of inflammatory bowel disease in a relevant mouse model, Eur. J. Pharm. Biopharm. 119 (2017 Oct) 361–371, https://doi.org/10.1016/j.ejpb.2017.07.004.
[114] Y. Chen, Y. Xiang, Efficacy of resveratrol for the treatment in patients with ulcerative colitis, Medicine 98 (46) (2019 Nov 1) e179388, https://doi.org/10.1097/MD.0000000000017938.